INTERRADICULAR MINERALIZED TISSUE ADAPTATION IN AN ASEPTIC NECROSIS MODEL

A report submitted in partial fulfilment of the requirement for the degree of Doctor of Clinical Dentistry (Orthodontics)

by

Andrew Chang
BDS (Hons)

Orthodontic Unit
Dental School
Faculty of Health Science
The University of Adelaide
2008

1.1 CONTENTS

1.1 CONTENTS…… 2
1.2 LIST OF FIGURES 5
1.3 LIST OF TABLES 8
1.4 LISTS OF GRAPHS 8
1.5 LIST OF ABBREVIATIONS 9
1.5.1 General 9
1.5.2 Units of measurements 9
2. ACKNOWLEDGEMENTS 10
3. SIGNED STATEMENT 11
4. SUMMARY 12
5. LITERATURE REVIEW 14
5.1 PERIODONTIUM 14
5.1.1 Definition 14
5.1.2 Elements 14
5.1.3 Features of the periodontium unique to rodents 34
5.2 DENTINE-PULP COMPLEX 35
5.2.1 Dentine types-Response of pulp to dental trauma 35
5.2.2 Pulp stones 37
5.3 ROOT RESORPTION 37
5.3.1 Classification of external root resorption 38
5.3.2 Histopathogenesis 39
5.3.3 Repair of resorption 41
5.4 PHYSIOLOGIC TOOTH MIGRATION 43
5.4.1 Bone Kinetics 43
5.4.2 Bone remodeling 44
5.5 ANKYLOSIS 51
5.5.1 Experimental models 52
5.5.2 Periodontal wound healing 53
5.5.3 Pathogenesis 55
5.5.4 Spatial distribution of ankylosis 58
5.5.5 Resorption and ankylosis 59
5.5.6 Transient ankylosis 61
5.6 BONE HISTOMORPHOMETRY 63
5.6.1 Applications 64
5.6.2 Bone Labels 65
6. RATIONALE OF THE CURRENT STUDY 69
7. AIMS 71
7.1 NULL HYPOTHESIS 71
8 MATERIALS AND METHODS 72
8.1 EXPERIMENTAL ANIMALS 72
8.2 ANAESTHESIA 73
8.3 THERMAL INSULT 75
8.4 BONE LABELS 76
8.5 SPECIMEN COLLECTION 77

8.6 TISSUE PROCESSING…….. 78
8.7 SELECTING REGION OF INTEREST- THE REPRESENTATIVE FURCATION 78
8.8 PILOT STUDY WITH MICRO-TOMOGRAPHY 80
8.9 BLOCK PREPARATION 82
8.10 SECTIONING 83
8.11 PROCESSING OF SECTIONS 84
8.11.1 Slide preparation & mounting 84
8.11.2 Staining 85
8.12 HISTOMORPHOMETRY 86
8.12.1 Unstained sections: 86
8.12.2 von Kossa counterstained with H&E sections 92
8.13 MICROSCOPIC IMAGING 93
8.14 STATISTICAL ANALYSIS 94
8.14.1 Mineral apposition rates and periodontal ligament width 94
8.14.2 Resorption 95
8.14.3 Method error 95
9. RESULTS 96
9.1 EXPERIMENTAL ANIMALS 96
9.2 ANAESTHESIA 96
9.3 MICRO-COMPUTED TOMOGRAPHY PILOT STUDY 97
9.4 SLIDES 99
9.4.1 General morphological observations 99
9.4.2 Day 7 100
9.4.3 Day 14 105
9.4.4 Day 21 114
9.4.5 Day 28 123
9.4.6 Polarized light 131
9.5 STATISTICAL ANALYSIS 133
9.5.1 Mineral Apposition rates (MAR) 133
9.5.2 MAR and label types 139
9.5.3 Periodontal ligament width 140
9.5.5 Resorption 142
9.5.5 Relationship between % surface resorption and % number of lacunae 148
9.5.6 Error study 148
10. DISCUSSION 150
10.1 METHODOLOGY 150
10.1.1 Sectioning, mounting and staining 150
10.1.2 Processing protocol 151
10.1.3 Orientation- determining the furcation region 152
10.2 MINERALIZED TISSUE LABELS 152
10.3 MINERAL TISSUE ADAPTATION 156
10.3.1 Bone 156
10.3.2 Pulp 158
10.3.3 Root 160
10.4 PERIODONTAL LIGAMENT WIDTH 163
10.5 TREATMENT AND SHAM RATS 164
10.6 ANKYLOSIS 164

10.7 CLINICAL IMPLICATIONS OF STUDY 167
10.8 AREAS OF FURTHER STUDY 168
11. CONCLUSIONS 169
12. APPENDICES 171
12.1 SPECIMEN PREPARATION 171
12.2 SLIDE PREPARATION AND SECTION PROCESSING PROTOCOL 172
12.2.1 Slide coating procedures for undecalcified bone sections 172
12.2.2 Slides with unstained sections- processing 172
12.2.3 Slides with undecalcified sections- processing for VK/H&E staining 173
12.2.4 Slides with decalcified sections- processing for H&E staining 174
12.3 STATISTICAL DATA 174
12.3.1 Histogram plot of MAR distribution 174
12.3.2 Histogram plot of log MAR distribution 175
12.3.3 Histogram plot of PDL width distribution 175
12.3.4 MAR dataset 176
12.3.5 Resorption dataset 178
13. REFERENCES 181

1.2 List of Figures

Figure 1. Elements of the periodontium 14

Figure 2. Photomicrograph showing detailed histologic characteristics of cancellous woven trabeculae labeled with tetracycline with their randomly oriented collagen fibres viewed under (A) UV light, (B) polarized light. Cancellous lamellar trabeculae with their orderly oriented collagen fibres viewed under (C) UV light, (D) polarized light. 21

Figure 3. Diagram illustrating experimental design in rats in the 4 observation periods 72

Figure 4. Digital scale balance used to record rat's weight 73

Figure 5. Isoflurane gas chamber 74

Figure 6. Inhalational sedation with isoflurane/oxygen mixture 74

Figure 7. Elevation of rat's skin and superficial muscles to improve intraperitoneal administration 75

Figure 8. Armamentarium for dry ice administration in rats 75

Figure 9. Anaesthetized experimental rat receiving dry ice to upper right first molar .. 76

Figure 10 Upper right 1st molar of a Sprague-Dawley rat. Buccal view. 79

Figure 11 Upper right 1st molar. Palatal view. 80

Figure 12 Diagrammatic view of occlusal surface of maxillary arch of male Sprague Dawley rat. [70]. 80

Figure 13 The SkyScan 1072, X-ray Micro-tomography system 81

Figure 14. Square grid of 1000µm length, used for quantification in unstained sections, positioned using the centre of the crown and periodontal ligament width as guides 89

Figure 15 Only surface labels measured and traced. Cropped 1000µm x1000µm grid from Figure 14. 91

Figure 16. 1000µm x1000µm grid used for semiquantification of von Kossa counterstained with H&E sections. Asterisks denote 'punched out' appearance along dentine surface used to identify resorptive surfaces. 93

Figure 17. Micro-CT coronal images from an experimental sham rat to illustrate coronal dental anatomy of the upper 1st molars. MP: Mesiopalatal, PP: Pulpal-periodontal, DB: Distobuccal, DP: Distopalatal. 98

Figure 18. Increased vascularity within the pulp chamber was a common finding in the treated molars. 101

Figure 19. Extensive surface bone and root resorption with a decreased cellularity (asterisks) in the periodontal ligament compared with the control molars.. . 102

Figure 20. Markedly less resorption along the root surface (arrows).. 102

Figure 21. Surface pitting on the root surface with an absence of active mineralization. 104

Figure 22. Distance of the label to its corresponding mineralized tissue surface was largest in alveolar bone, much less along the pulpal floor and least along the root surface. 104

Figure 23. Similar rank order of appositional activity (as in Fig 22) also seen in controls. 105

Figure 24. Root resorption with repair cellular cementum-like tissue formation on the root surface, concurrent with marked localized cellular and vascular changes in the pulp, including bone-like tissue 107

Figure 25. A discontinuous layer of of odontoblast-like cells (arrows) lying deep to a wide layer of unmineralized predentinal matrix (asterisk) 107

Figure 26. Bone-like tissue(**) in pulp chamber surrounded by hematoxyphilic cells. 108

Figure 27. Signs of rapid repair of resorption along the bone and root surface 14days after thermal insult with haphazard arrangement of periodontal ligament collagen fibres. 108

Figure 28. Unattached mineralized nodule within the periodontal ligament space of the same rat. Unlabeled arrow denotes cellular cementum-like tissue on root surface. 109

Figure 29. Deposits of unmineralized matrix along the bone, root surfaces and in the body of the ankylotic region (arrows). 109

Figure 30. Ankylosis with increased cellularity and vascularity in the periodontal ligament. 110

Figure 31. Focal type of ankylosis with rapid apposition across the periodontal ligament space. 112

Figure 32. Finger like projections from the root surface (unlabeled arrows) with an absence of label uptake along the root surface. 113

Figure 33. Ankylosis but no label uptake.. 113

Figure 34. Sham control rat. Mineral apposition greatest along alveolar bone surface with an absence of mineralization along the root surface. 114

Figure 35. Ankylosis with deposits of unmineralized matrix (unlabeled arrows) along its peripheries. 116

Figure 36. Cellular cementum-like material (arrows) on the root surface. 116

Figure 37. Rat 4- No ankylosis but irregular extensions from bone and root surface (black arrows) and bone –like tissue (blue arrows) within the middle of the periodontal ligament and along the walls of the pulp. 117

Figure 38. An irregular root surface (asterisks) characteristic of resorption, and a rim of odontoblast-like cells, when seen under higher power, lining the walls of the pulp (broken arrow). 117

Figure 39. Cellular-like cementum absent from root surface. 118

Figure 40. Focal region of ankylosis. Active mineral apposition present on the surface of the ankylotic body and along its immediately connecting bone and root surfaces. 120

Figure 41. Mineralization (arrow) within the middle of the periodontal ligament space. 121

Figure 42. Mineralization of reactive hard tissue which corresponded with cellular-like cementum tissue when stained sections were viewed under transmitted light. 121

Figure 43. An irregular root surface characteristic of resorption and mineralization of alveolar bone nodular extensions (arrows) within the middle of the periodontal ligament space. 122

Figure 44. Minimal appositional activity along the root and pulpal surface in control left molar. 122

Figure 45. Fewer blood vessels in the pulp compared with earlier time periods (Figs 18 and 24), lined by a rim of odontoblast-like cells (white arrow), which lie beneath a wide zone of reactive hard tissue. 124

Figure 46. An organized, cellular periodontal ligament, with a rim of cells lining the root and bone surfaces (black arrows). 125

Figure 47. A cellular pulp with an irregular root surface (asterisks) characteristic of resorption. 125

Figure 48. Absence of cellular-like cementum on root surface with organized arrangement of collagen fibres (green asterisks) in the periodontal ligament. 126

Figure 49. A cellular periodontal ligament with a layer of acellular cementum (arrow) lining the root surface of the control molar 126

Figure 50. Smooth root surface (white arrows) suggestive of an absence of resorption, and a lining of cells along the the bone, root and pulpal surfaces (black arrows) 127

Figure 51. Less irregular root surface (broken arrows) compared with Days 7, 14 and 21, with mineral apposition in the pulp (unbroken arrow). 129

Figure 52. An irregular root surface characteristic of resorption lacunae (broken arrow) along the root surface which did not accumulate label. 129

Figure 53. Largest mineral apposition within the alveolar bone. Similar rank order of appositional activity amongst bone, pulp and root surfaces with two labels, as with one label in Fig 22. 130

Figure 54. 1000µm x 1000µm region of interest. No differences in the pattern of polarization across the 3 categories: within the ankylotic body (arrow, Fig A), alveolar bone (white asterisks, Figs A, B, C), and mineralized tissue on root surface in treated rats (red asterisks, Figs A, B)
A. Day 14, Rat 3. Right molar. Unstained
B. Day 21, Rat 5. Right molar.Unstained
C. Day 14, Sham rat. Left molar. Unstained 133

1.3 List of Tables

Table 1. Distribution of ankylosis in experimental rats 100
Table 2. Distribution of labels among rats in Group 1 (7 days) 103
Table 3. Distribution of labels among rats in Group 2 (14 days) 111
Table 4. Distribution of labels among rats in Group 3 (21 days) 118
Table 5. Distribution of labels among rats in Group 4 (28 days) 127
Table 6. Results of multivariate analysis of the MAR data from all rats* 134
Table 7. Dataset for mean MAR_{bone} on left and right first molars 136
Table 8. Dataset for mean MAR_{root} on left and right first molars 137
Table 9. Dataset for mean MAR_{pulp} on left and right first molars 138
Table 10. Differences of adjusted means for 3 label types. 139
Table 11. Mean MAR for the 3 different label types 139
Table 12. Results of multivariate analysis of PDL width from all rats 140
Table 13. Dataset for mean PDL width 141
Table 14. Variables influencing mean % resorptive surface ($R_{bone\ or\ root}$) 142
Table 15. Dataset for mean % resorptive surface 143
Table 16. Dataset for mean % surface root resorption 144
Table 17. Variables influencing mean % lacunae number 145
Table 18. Dataset for mean % lacunae number for bone (NL_{bone}) 146
Table 19. Dataset for mean % lacunae number for root (NL_{root}) 147
Table 20. Interaction between $R_{bone\ or\ root}$ and $NL_{bone\ or\ root}$ 148

1.4 Lists of Graphs

Graph 1. Mean MAR (and SE) on bone surfaces for left and right first molars 135
Graph 2. Mean MAR (and SE) on root surfaces for left and right first molars 137
Graph 3. Mean MAR (and SE) on pulpal surfaces for left and right first molars 138
Graph 4. Mean PDL width for left and right first molars 141
Graph 5. Mean surface bone resorption (and SE) on left and right first molars 143
Graph 6. Mean surface root resorption (and SE) on left and right first molars 144
Graph 7. Mean % lacunae number (and SE) on bone for left and right first molars 146
Graph 8. Mean % lacunae number (and SE) on root for left and right first molars 147

1.5 List of abbreviations

1.5.1 General

H&E- haematoxylin and eosin

VK/H&E- Von Kossa counterstained with haematoxylin and eosin.

BMU- basic multicellular unit

IMVS- Institute of Medical and Veterinary Sciences

Ver- version

CT- computerized tomography

MAR- mineral apposition rates

PDL- periodontal ligament

ID- identification number

Z- coronal plane notation adopted by Dataviewer v1.3.2 (a Skyscan 1072 application software)

SE- standard error

1.5.2 Units of measurements

µm- micrometres

px- pixel

2. ACKNOWLEDGEMENTS

I wish to express my appreciation and thanks to the following people for their invaluable assistance in the completion of this thesis.

Professor Wayne Sampson, P.R. Begg Chair in Orthodontics, University of Adelaide, for his expert advice, guidance and editorial opinion throughout this project.

Professor Nick Fazzalari, Head of Bone and Joint Research Laboratory, Division of Tissue Pathology, Institute of Medical and Veterinary Science, Adelaide, for his expert advice, guidance and editorial opinion throughout this project.

Bone and Joint Research Laboratory staff- Bingkui Ma, Helen Tsangari, Vivienne Le and Ian Parkinson for their assistance in design of this project, instructions in the use of specialized microtome instruments, histological techniques and staining and use of histomorphometric software.

Dr Craig Dreyer, Senior Lecturer in Orthodontics, University of Adelaide, for his instruction and assistance in the techniques used in this study as well as useful feedback.

Mr Thomas Sullivan, Department of Public Health, University of Adelaide, for his expert assistance with statistical analysis.

Ms Sandie Hughes, for her assistance during the laboratory stages of this project.

To my wife Sherry for her constant support and encouragement throughout the past three years and to my daughter Amelia, her constant smiles and laughter make everything worthwhile.

3. SIGNED STATEMENT

This report contains no new material that has been accepted for the award of any other degree or diploma in any other university. To the best of my belief, it contains no material previously published except where due reference is made in the text.
I give consent for this copy of my thesis, when deposited in the University library, to be made available for loan and photocopying.

Andrew Chang

4. SUMMARY

Key Words:

Ankylosis, Resorption, Labels, Periodontal Ligament, Rats

This study used vital bone markers to investigate mineralized tissue adaptation in the periodontium of rats after a hypothermic insult to their maxillary first molars. This hypothermic insult has been shown in previous studies to induce aseptic root resorption with variable effects on ankylosis. A secondary objective was to assess the pulpal changes that occurred concurrent with the changes in the periodontium.

Four groups of 7, eight-week old male Sprague Dawley rats were assigned to be euthanased at the day 7, 14, 21 and 28 observation periods. At day 0, 4 groups of 6 rats were subject to a single 20 minute application of dry ice on their maxillary right first molar. The remaining 1 rat within each group did not receive the dry ice. All rats were given 2 sequential bone labels, calcein 5mg/kg and alizarin red 30mg/kg, administered intraperitoneally 8 days apart. The timing of the labels was such that all rats were euthanased 2 days after the last label. The rat maxillae were fixed in ethanol and embedded undecalcified in methylmethacrylate. Ten micrometre coronal sections were obtained through the furcation of the first molars with three of each group of ten consecutive sections being unstained, stained with von Kossa/ hematoxylin and eosin counterstain, or decalcified and stained with hematoxylin and eosin, respectively. Unstained sections were viewed under fluorescence, while transmitted light microscopy was used for the other sections. Mineral apposition rates along the bone, root and pulpal surfaces as well as periodontal ligament width were measured using histomorphometry. Semiquantitative measurements of the resorptive surfaces within the periodontium were

also noted. Multivariate and negative binomial regression statistical analyses were used to identify influencing variables.

A focal pattern of ankylosis was observed at days 14 and 21 in 3 rats and was not seen at day 28. In both the treated and control teeth, appositional activity was greatest along bone and least along the root surface. Mineral tissue apposition rates along the bone and root surface displayed an initial spike during day 14 but declined to levels of the control teeth by day 28. A longer time lag was observed with appositional activity in the pulp which also displayed a declining trend towards the control teeth values by day 28. Resorption levels along the root surface continued to remain significantly ($p<0.0001$) elevated. The significantly ($p<0.0001$) wider periodontal ligament width in the treated molars showed a declining trend towards that of the control teeth by day 28.

There was a temporary disturbance of mineralized tissue adaptation on the bone and root surfaces with a recovery of cellular vitality within the periodontium and pulp and a trend towards homeostasis of the periodontal ligament width. The null hypotheses that a single prolonged thermal insult on a rat has no effect on mineralized tissue adaptation within the periodontium and pulp chamber and that the periodontal ligament width within the interradicular region does not change in response to thermal trauma induced by the present study were rejected.

5. LITERATURE REVIEW

5.1 PERIODONTIUM

5.1.1 Definition

Periodontium is a collective term defined as the tissues which invest and support the teeth (Fig 1) [1].

5.1.2 Elements

1. Root cementum (C)
2. Alveolar bone (E)
3. Periodontal ligament (F)
4. Gingiva (G)

Figure 1. Ground coronal section of a human premolar tooth, and elements of the periodontium: C, E, F and G. Adapted from Berkovitz [2]

5.1.2.1 Cementum

Cementum is an avascular mineralized tissue usually covering the entire root surface. The main function of cementum is to anchor the principal collagen fibres of the PDL to the root surface. It also has important adaptive and reparative functions, playing a crucial role to maintain occlusal relationships and to protect the integrity of the root surface [3, 4]. Root

cementum is avascular, non-innervated, does not undergo continuous remodeling like bone and continues to grow in thickness throughout life [3, 5, 6]. At the cemento-enamel junction, cementum forms a thin layer that becomes thicker towards the apex of the root [7].

Cementum is critical for the appropriate maturation of the periodontium, both during development as well as that associated with the regeneration of periodontal tissues [5]. Bone formation and possibly formation of apical cementum are adaptations to a slow eruptive movement throughout the life of the tooth [8, 9].

5.1.2.1.1 Classification

Light and electron microscopy has enabled cementum to be classified into 2 basic types based on the presence (cellular) or absence (acellular) of cells and the source of collagen fibres (extrinsic versus intrinsic) [5, 6, 10].

These are:

1) Acellular extrinsic fibre cementum (AEFC) is found in the cervical half to two-thirds of the root. It develops very slowly and is considered acellular as the cells that form it remain on the surface. The matrix consists of noncollagenous proteins elaborated by the cementoblasts and of extrinsic collagen fibres formed by the PDL fibroblasts which has an important role in tooth attachment [7].

The orientation of the Sharpey's fibres is subject to changes throughout life, due to post-eruptive tooth movement. These changes in orientation are reflected by individual AEFC layers that are interfaced by growth, resting, or incremental lines. AEFC grows very slowly, but at a fairly constant rate. The slow rate of formation, the absence of cementocytes, and the densely aggregated and parallel-oriented Sharpey's fibres account

for the very uniform morphological appearance of the AEFC and make it a unique tissue [11].

2) Cellular intrinsic fibre cementum (CIFC) is distributed along the apical third to half of the root and is found in furcation areas. The collagen fibrils of CIFC are intrinsic as they are formed by cementoblasts and do not protrude from cementum into the PDL space with no direct function in tooth attachment [11]. The intrinsic collagen fibres and the presence of cementoblasts entrapped in lacunae within the matrix they produce (cementocytes) are the characteristic features of cellular intrinsic fibre cementum [6]. In rodent molars during cellular cementum formation, initial cellular intrinsic fibre deposition is associated with the simultaneous formation of extrinsic fibres. When the cementoblasts move away from the cementum surface or are embedded in the cementum, these cells retract the processes that have encircled the principal fibres. At the same time, these cells secrete intrinsic fibres around the principal fibers. This results in the typical intrinsic-extrinsic fibre structures which in the early stages, has an irregular arrangement [12].

CIFC participates in the repair process of previously resorbed roots as only this type of cementum can fill a resorptive defect in a reasonable period of time [6, 13]. The rapid speed of formation and the presence of cells and lacunae may be the reason why this cementum variety is less well mineralized than AEFC. The structural organization of the cementum matrix and the presence of cells in it give cellular intrinsic fibre cementum a bone-like appearance [6].

Cellular mixed stratified cementum (CMFC) is found in humans in the apical one- to two-thirds of roots and the furcations. This comprises a stratification of consecutively

deposited, alternating layers of acellular extrinsic fibre cementum and cellular intrinsic fibre cementum that are unpredictably superimposed on one another. The intrinsic part of CMSC may exert an adaptive function, while the extrinsic part may contribute to tooth anchorage to the surrounding alveolar bone [11]. When the extrinsic fibres are continuous with the functionally oriented principal fibres of the PDL, they can be regarded as Sharpey's fibres. As layers of acellular extrinsic fibre cementum and cellular intrinsic fibre cementum develop unpredictably in time, space and thickness, particular root surface areas may temporarily remain unsupported by PDL fibres [3].

CMSC is not found in rodent molars but is always found in human teeth. The mineral density of CMSC is similar to bone [6].

5.1.2.1.2 Biochemical composition

The composition of cementum resembles that of bone. It contains about 50% mineral (substituted apatite) and 50% organic matrix. Type I collagen is the predominant organic component, constituting up to 90% of the organic matrix. Other collagens associated with cementum include type III, a less cross-linked collagen found in high concentrations during development and repair/regeneration of mineralized tissues, and type XII, a fibril-associated collagen that binds to type I collagen and also to noncollagenous matrix proteins. The noncollagenous matrix proteins are similar in bone and cementum. They fill in the spaces between the collagen fibrils, regulate mineral deposition and impart cohesion to the mineralized layer [6].

5.1.2.1.3 Physiological changes

Cementum thickness depends on a variety of factors including tooth shape, eruptional and functional history, and age. The actual contribution of any of these factors is still ill-defined [10].

Concave root aspects facing the furcations of human maxillary and mandibular first molars show thicker cementum than adjacent convex root aspects [14].

In humans, a linear relationship between cementum thickness and age in single-rooted teeth possibly reflects continuous cementum apposition throughout their lifespan [15].

In the molar teeth of rats, the rate of cementum apposition is greater in young than in mature and old animals. Cementum deposits are thicker in the interradicular and periapical regions of the molars, which continue to erupt and change their position relative to bone throughout their lifespan [16]. Apical cementum apposition in these teeth is believed to compensate for occlusal wear [10]. One other factor contributing to cementum thickness in the mid-root, interradicular and apical regions of the tooth may be its past history of eruption, involving axial shifts as well as rotational movements [10, 16].

No morphologically distinct layer of cementoid, akin to osteoid or predentine, exists on the surface of acellular extrinsic fibre cementum. In contrast, for cellular intrinsic fibre cementum, a layer of unmineralized matrix (cementoid) is established at the surface of the mineralized cementum matrix, with the mineralization front at the interface between the two layers. In contrast to osteoid, cementoid is not as regular and readily discernible [6].

5.1.2.2 Alveolar bone

Alveolar bone may be defined as the part of the maxilla or mandible which supports and protects the teeth [2]. The presence of an alveolar bone along the entire tooth socket separates the support bone anatomically and functionally from the PDL [6]. Alveolar bone comprises the alveolar process, which is an extension of the basal bone of the jaws. The alveolar bone forms in relation to the teeth, but structurally it is similar to, and continuous with, the basal bone [17].

5.1.2.2.1 Composition

1. Compact (cortical) bone. These are the outer buccal, lingual and palatal cortical plates. The cortical plates consist of circumferential layers (lamellae) of fine-fibred bone supported by Haversian systems. The lamellae are arranged concentrically around channels containing one or more blood vessels (Volkmann's canals).
2. Cancellous (trabecular) bone. This occupies the central part of the alveolar process and consists of bony trabeculae with yellow marrow rich in adipose cells filling the intertrabecular spaces. The trabeculae also contain lamellae which are roughly parallel to the bone surface.
3. The alveolar wall. This bone lining the tooth socket is specifically known as bundle bone as it provides attachment for the PDL fibres [6, 18]. This consists of successive layers of intrinsic fibre bundles running more or less parallel to the socket. Embedded within this bundle bone, almost perpendicular to its surface, are the extremities (Sharpey's fibres) of the extrinsic collagen fibre bundles of the PDL, which are mineralized only at the periphery.

The composition of the extracellular matrix of alveolar bone appears to be similar to other bone tissues [17]. The bone matrix is formed from a scaffold of interwoven collagen fibres within and between which small, uniform, plate-like crystals of carbonated hydroxyapatite $\{Ca_{10}(PO_4)_6(OH)_2\}$ are deposited. Proteoglycans, acidic glycosylated and non-glycosylated proteins associate with and regulate the formation of collagen fibrils and mineral crystals, or provide continuity between matrix components and between the matrix and cellular components. Small amounts of carbohydrate and lipid contribute to the organic matrix, which comprises approximately one-third of the matrix while the inorganic components account for the remaining two-thirds.

Collagen comprises the major (approximately 80%-90%) organic component in mineralized bone tissues. Type I collagen (>95%) is the principal collagen in mineralized bone.

5.1.2.2.1.1 Woven bone

Woven bone and lamellar bone are the two sub-tissue types in the skeletal tissue based on the organization of collagen fibres within the bone matrix [19]. The immature woven bone is formed rapidly during early development and in repair sites. Because of the rapid formation, the interwoven coarse collagen fibres are arranged in a disorganized, random fashion (Fig 2A, B). The distribution of osteocytes generally follows that of the collagen fibre and is also in a random fashion. This results in the rapid formation of a temporary functional structure to partially restore mechanical properties, such as stiffness. The loading condition initiates secondary bone remodeling, replacing the woven bone callus with lamellar bone. In all cases, woven bone is considered an interim material that is resorbed and replaced by lamellar bone. The mechanical strength of woven bone is weak

due to its randomly oriented and loosely bundled collagen fibres and low mineral deposition.

5.1.2.2.1.2 Lamellar bone

Lamellar bone is formed at a much slower rate. The collagen fibres produced during bone formation are laid onto the existing bone surfaces in an orderly fashion (Fig 2C, D). The collagen fibres made by osteoblasts are laid down layer by layer with strict organization. For each layer, collagen fibres are laid parallel to each other, forming a bone matrix sheet, which is called a lamella. In the next layer, the direction of the collagen fibres is perpendicular to that of the previous layer. As such, the histological appearance of this lamination under polarized light is alternating light-dark layers, representing the cross-sectional and longitudinal oriented collagen fibres on the histologic section. The mechanical strength of lamellar bone is strong due to its orderly, oriented, stably-bundled collagen fibres and high mineral deposition.

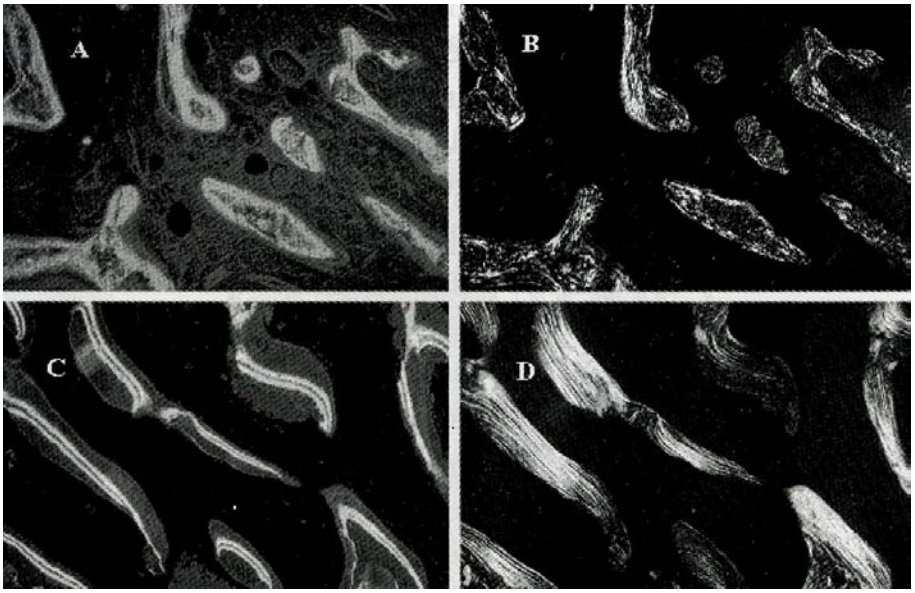

Figure 2. Photomicrograph showing detailed histologic characteristics of cancellous woven trabeculae labeled with tetracycline with their randomly oriented collagen fibres viewed under (A) UV light, (B) polarized light. Cancellous lamellar trabeculae with their orderly oriented collagen fibres viewed under (C) UV light, (D) polarized light. Adapted from Xiao et al [19].

5.1.2.2.2 Function

Alveolar bone is specialized for tooth support, with a rapid rate of turnover and loss in the absence of a tooth. This facilitates positional adaptation of teeth in response to functional forces and the physiological occurances (such as mesial drift of teeth in humans and primates and bucco-distally in rodents) and tooth eruption that occurs with the development of the jaw bones [1, 17, 18]. It also serves as a major reservoir of calcium [11].

5.1.2.2.3 Anatomy and microstructure

As a result of physiological tooth movement, the tooth socket is spatially oriented: the side of the socket in the direction of migration is irregular and scalloped by numerous lacunae of various lengths and depths (the resorbing side), while the opposite side is regular and smooth (the apposition side). On the resorbing side of the tooth socket, as part of bone remodeling, resorption, reversal and formation phases may be identified [18, 20].

The bundle bone consists of successive layers of coarse-fibred woven bone fibres running parallel to the socket wall and arranged in lamellae [7]. It is thin and ranges between 100μm and 200μm in humans. The bundle bone may appear thicker on one side of the socket (the apposition side), but only its outer layer is functional, with the presence of regularly spaced cement lines which interrupts the course of the extrinsic fibres [18]. Embedded within this bundle bone, perpendicular to its surface, are the extremities (Sharpey's fibres) of the extrinsic collagen fibre bundles of the PDL. When bundle bone has reached a certain thickness and maturity, parts of it are reorganized into lamellated bone, with finer fibrils in its matrix [21].

The cortical plates and bone lining the alveolus meet at the alveolar crest. The cortical plates consist of surface layers (lamellae) of fine-fibre bone supported by Haversian systems. The trabecular bone occupying the central part of the alveolar process also consists of bone disposed in lamellae, with Haversian systems present in the larger trabeculae. Yellow marrow, rich in adipose cells, generally fills the intertrabecular spaces [6].

5.1.2.2.4 Osteogenic Cells

Bone formation, maintenance and resorption are regulated by osteoclasts, osteoblasts, osteocytes and bone-lining cells.

5.1.2.2.4.1 Osteoclasts

While the primary resorptive cell is the osteoclast, macrophages[22] and moncytes[23] are also able to resorb mineralized tissues. Osteoclasts are large, multinucleated, highly motile cells formed by the fusion of mononuclear precursor cells of hematopoietic origin [17]. Osteoclasts have a diameter ranging from 20µm to more than 100µm in diameter and normal osteoclasts contain up to 10 nuclei. They are the principal bone-resorbing cells, responsible for the degradation and removal of the inorganic and organic components of the bone matrix [24].

Osteoclasts are relatively sparsely distributed in bone. In their differentiation process, hematopoietic stem cells give rise to circulating mononuclear cells called colony forming unit-granulocyte/macrophages (CFU-GM). M-CSF (Macrophage-colony stimulating factor) supports the proliferation of CFU-GM and keeps the mononuclear cells in

monocyte/macrophage lineage. The mononuclear precursors are attracted to prospective resorption sites through chemotactic stimuli and they attach onto bone matrix to further differentiate into prefusion osteoclasts with the stimulation of M-CSF and RANKL {Receptor Activator of nuclear factor-kappa (NF-κB) ligand}. These bind to the RANK receptor on the osteoclast surface. The binding of RANKL to RANK activates multiple signal transduction pathways that commit the differentiation of the precursor cells. Osteoblasts support this differentiation process by serving as a source of M-CSF and RANKL. In the continuing presence of these 2 factors, the prefusion osteoclasts continue to differentiate by fusion to become multinucleated cells. RANKL is also necessary in the further activation of the multinucleated osteoclasts by stimulation of the ruffled border membrane, which has numerous pumps that transport protons into the resorption compartment of the osteoclast to maintain a low-pH environment. Dissolution of inorganic components of bone is followed by the degradation of organic components of bone, through the action of proteolytic enzymes which are released through the ruffled border membrane. Only the cells in the later stages of the differentiation process, the prefusion osteoclasts, the multinucleated osteoclasts and the activated osteoclasts possess tartrate resistant acid phosphatase, which is the most widely used marker for osteoclasts [24].

The activated multinucleated osteoclasts represents the end point of a differentiation process and are not themselves capable of proliferation [25]. The lifespan of an osteoclastic nucleus is approximately 10-12.5 days. Upon completion of their resorptive function, they migrate into the marrow space, ultimately undergoing apoptosis, characterized by nuclear and cytoplasmic condensation and fragmentation of nuclear DNA [19, 26].

5.1.2.2.4.2 Osteoblasts

Osteoblasts are 15-30µm, cuboidal or columnar cells of mesenchymal origin that typically form a single layer that covers all periosteal or endosteal surfaces where bone formation is active. They are the most active secretory cells in bone and are primarily responsible for the synthesis and secretion of collagen that forms the unmineralized matrix (osteoid). They also participate in osteoid calcification by regulating the flux of calcium and phosphate in and out of bone [17, 19, 25]. Their nucleus is round, and when active, their cytoplasm is filled with a prominent Golgi complex and abundant rough endoplasmic reticulum.

Mesenchymal stem cells in the bone marrow or connective tissue are the primary cell source from which osteoblasts are derived. Other sources of these skeletal stem cells include vascular pericytes, periosteum, adipose tissue, amniotic fluid, umbilical cord blood and adult peripheral blood [27]. There are many factors which control the differentiation of mesenchymal stem cells into osteoblasts, among which include Runx2, Indian Hedgehog (in endochondral bone), and genes belonging to the BMP (bone morphogenetic proteins) superfamily [26]. Osteoblasts are terminally differentiated cells, and the possible fates of an active osteoblast are to become a bone lining cell, an osteocyte, or apoptosis [19]. Osteoblasts positively regulate the differentiation and function of osteoclasts, through the RANK/RANKL pathway. However, they also negatively regulate osteoclastogenesis though osteoprotegerin (OPG), which is widely expressed by osteoblasts [28]. This acts as a decoy receptor to compete with RANK for RANKL.

In areas of active bone remodeling, typical osteoblasts lay down bone matrix over a densely stained reversal line [18]. Active osteoblasts secrete type I collagen, the principal organic component of bone matrix, along with a variety of non-collagenous proteins which make up to 5 per cent of the organic matrix; including osteocalcin, phosphorylated glycoproteins, bone sialoproteins and proteoglycans. Expression of alkaline phosphatase by osteoblasts appears to reflect bone formation activity, but the precise function of this enzyme in bone is unknown [25], although it may play an important role in osteoid mineralization [29].

5.1.2.2.4.3 Osteocytes

This is the most abundant cell type in bone tissue. In mature bone, about 95% of total bone cells are osteocytes. Osteocytes are the only cell type to be embedded within the bone matrix [19].

Following maturation, osteoblasts may undergo apoptosis, become progressively encased in osteoid and then mineralized matrix as osteocytes or remain on the bone surface as bone lining cells [17]. Osteoblasts that become osteocytes occupy spaces (lacunae) in bone and are defined as cells surrounded by bone matrix, whether mineralized or still part of the osteoid seam. Osteocytes are smaller cells than osteoblasts, and have a decreased quantity of synthetic and secretory organelles, with the nucleus occupying a significantly larger proportion of the cell. A major feature of osteocytes is the presence of numerous and extensive cell processes that ramify throughout the bone in canaliculi and make contact, frequently via gap junctions, with processes from other osteocytes or with similar processes extending from osteoblasts or bone lining cells at the surface of bone [17]. Many osteocytes eventually undergo apoptosis [19].

The physiological function of the osteocyte with its 3D network throughout bone is hypothesized to be the regulation of the exchange of mineral ions between interstitial fluid and extracellular fluid, working with the osteoblasts and maintaining a local mineral ionic environment that is suitable for bone matrix mineralization [19]. While matrix formation takes place at the interface between osteoblasts and osteoid, mineralization occurs at the interface between osteoid and the mineralized bone, the mineralization front.

5.1.2.2.4.4 Bone-lining cells

The third cell type belonging to the osteoblast family, the bone-lining cells, are also known as resting osteoblasts. Bone lining cells are about 1μm thick with a 12μm diameter, with a thin, flat nucleus and attenuated cytoplasm. They appear as a near confluent, flattened single layer over quiescent bone surfaces [25]. These cells have a reduced capacity for protein secretion with a relative paucity of organelles.
Bone-lining cells are derived from surface osteoblasts when they have completed their historical role as bone forming cells. The ultimate fate of bone-lining cells is presumable death by apoptosis [17]. They are connected to one another and to the osteocytes.

In response to an activation signal from osteoblasts, the bone-lining cells contract, releasing proteases that digest the underlying osteoid, exposing the mineralized surface for osteoclastic resorption [19].

During the quiescent period, bone lining cells, together with a 1μm underneath layer of osteoid, serve as a barrier to protect bone surfaces from inappropriate resorption by

osteoclasts or other inflammatory cells [24]. These cells cover most quiescent bone surfaces in the adult skeleton which are a primary site of mineral ion exchange between blood and adult bone. Together with osteocytes, bone lining cells and their connecting cell processes appear to form a homeostatic network of cells capable of regulating the plasma calcium concentration.

5.1.2.2.4.5 Skeletal adaptation

Both cortical and trabecular bone grow, adapt and turnover by means of two fundamentally different mechanisms: modeling and remodeling [30]. In bone modeling, independent sites of resorption and formation change the form (shape or size or both) of bone. In bone remodeling, a specific coupled sequence of resorption and formation occurs to replace previously existing bone. Bone modeling is the dominant process of facial growth and adaptation to applied loads such as headgear, rapid palatal expansion, and functional appliances. Modeling changes can be seen on cephalometric tracings, but remodeling events, which usually occur at the same time, are apparent only at the microscopic level.

5.1.2.3 Periodontal ligament

The periodontal ligament (PDL) is a highly vascular and cellular connective tissue situated between the cementum covering the root of the tooth and the bone forming the socket wall. It ranges in width from 0.15 to 0.38 mm in humans, with its thinnest portion around the middle third of the root, showing a progressive decrease in thickness with age [6].

There are species variations in the PDL. In mice, the width of the PDL has been found to be uniform around the mesial root of the lower first molar in both young and old mice

throughout the apico-occlusal length of the root [31]. The PDL volume in rats around buccal roots of the lower first molar also maintain a constant volume during distal drift [20].

5.1.2.3.1 Function

The principal function of the PDL is to anchor the tooth root to the jaw bone and to distribute multidirectional mechanical stresses such as masticatory forces [1]. The PDL also contain sensory receptors necessary for the proper positioning of the jaws during mastication and provides a cell reservoir for tissue homeostasis and repair/regeneration [6].

5.1.2.3.2 Composition

As with all connective tissues, the PDL consists of many differentiated cells, their precursors and an extracellular compartment comprising collagenous and noncollagenous matrix constituents [32]. In addition, the PDL has a unique vascular arrangement, lymphatic system and highly specialized network of nervous elements [1] that will not be discussed here.

5.1.2.3.3 Cellular elements

The differentiated cells include synthetic cells (osteoblasts, fibroblasts and cementoblasts), resorptive cells (osteoclasts, fibroblasts, odontoclasts), epithelial cells (epithelial cell rests of Malassez and endothelial cells), as well as miscellaneous connective tissue cells (mast cells, macrophages, neural cells etc) [1].

Odontoclasts have certain similar morphological features compared with osteoclasts.

These cells show multinucleation, and usually have ruffled borders at resorption sites, clear zones, abundant mitochondria, scattered rough endoplasmic reticulum, and tartrate-resistant acid phosphatase (TRAP) activity. These cells eventually undergo apoptosis with either spontaneous degeneration of the apoptotic bodies or phagocytosis by macrophages. Unlike osteoclasts, the lifespan of odontoclasts is not known [33]. TRAP positive multinucleated odontoclast cells attached to the root surface of resorption lacunae can appear as mononuclear depending on the plane of section [34]. TRAP positive mononuclear cells have also been identified adjacent to resorptive surfaces [35] with a low frequency of distribution [36], which commonly fuse together to form TRAP positive multinucleated clast-like cells [37]. However, it is not known the extent to which older and newer nuclei mix simultaneously during cell fusion with newly formed mononuclear odontoclasts, and if a relationship exists between the age of the nucleus and the degeneration of multinucleated odontoclasts, although Domon et al [33] only observed apoptosis present in TRAP positive odontoclasts with three or fewer nuclei.

Odontoclasts have fewer nuclei and are smaller than the osteoclasts[36]. They have very small or no clear zones in contrast to the well-developed clear zones of actively resorbing osteoclasts. This has been attributed to the difference in composition of the dental tissues when compared with bone [38].

Odontoclasts have not been determined to be osteoclast-type cells. In addition, both the origin and differentiation system of odontoclasts are unclear although it is postulated that odontoclast cells may be derived from mononuclear precursor cells from the hematopoietic system, similar to osteoclast cells [34].

As the fibroblast is the principal cell type in the PDL, it plays a significant role in normal turnover, repair, and regeneration [39]. The fibroblasts of the PDL are characterized by their rapid turnover of collagen.

5.1.2.3.4 Extracellular matrix

The extracellular compartment consists mainly of well-defined collagen fibre bundles embedded in an amorphous background material, known as ground substance [6, 39]. Collagen is the principal protein found in the PDL. Type I collagen is the major collagen type found and accounts for approximately 80% of PDL collagen. Type III collagen is the second most common collagen found. Both type I and type III collagen are uniformly distributed within the PDL [32].

The vast majority of collagen fibrils in the PDL are arranged in definite and distinct fibre bundles, and these are termed principal fibres. The extremities of collagen fibre bundles are embedded in cementum or bone. The embedded portion is referred to as Sharpey's fibres. Sharpey's fibres in primary acellular cementum are fully mineralized. Those in cellular cementum and bone are generally only partially mineralized at their periphery [6]. Oxytalan fibres occupy 3% of the volume of the periodontal ligament and extend the length of the ligament in an apico-occlusal direction. The oxytalan fibres fibres are numerous and dense in the cervical region of the ligament and are hypothesized to act to regulate vascular flow in relation to tooth function. There are no mature elastin fibres in the human PDL [7].

5.1.2.3.5 Origin of cementoblasts, osteoblasts & fibroblasts

It is not known whether distinct precursor cell lines exist for PDL fibroblasts, cementoblasts, and osteoblasts or whether these cells arise from a common precursor [6].

Classically, the dental follicle, with a possible contribution from the perifollicular mesenchyme, gives rise to PDL fibroblasts, osteoblasts, and cementoblasts [40].

In rodents, cementogenesis begins with the deposition of a matrix on the dentine surface by Hertwig's epithelial root sheath (HERS), disruption of the HERS, migration and organization by ectomesenchymal cells from the dental follicle, and their subsequent differentiation into cementoblasts [41].

A recent literature review supports the concept that cementoblasts producing both acellular extrinsic fibre cementum and cellular intrinsic fibre cementum are unique phenotypes that differ from osteoblasts [11]. It proposes a model that cells derived from HERS (Hertwig's epithelial root sheath) play an essential role in tissue development and maintenance. Cells descending from HERS may give direct rise to cells that form new cementum and PDL tissues, or play an indirect role by producing the necessary signaling molecules for cell recruitment and differentiation [6].

There is increasing evidence that the epithelial rests of Malassez, which are remnants of HERS are more than just a vestigial structure in the PDL [42]. These epithelial rests of Malassez are also likely involved in reparative cementogenesis [43, 44].

5.1.2.3.6 Physiologic regulation of the periodontal ligament space

The PDL also has the adaptive capacity to respond to functional changes. When the functional demand increases, the width of the PDL can increase by as much as 50%, and the fibre bundles also increase markedly in thickness. Conversely, a reduction in function leads to narrowing of the ligament and a decrease in number and thickness of the fibre bundles. These functional modifications of the PDL are associated with corresponding adaptive changes in the adjacent cementum and alveolar bone [6]. The surrounding alveolar bone rarely colonizes the PDL space. However, the limited but constant

physiological drift and eruption of mammalian teeth requires remodeling of the tissues of the periodontium [20].

The failure of homeostatic mechanisms to regulate PDL width has been implicated in tooth ankylosis, a condition in which the tooth root fuses to the bone. Certain non-physiological conditions can manifest with the destruction of the PDL and ankylosis, suggesting that the regulatory mechanisms for the maintenance of the PDL width are expressed by PDL cells [45]. In vivo studies have underlined the active role of PDL fibroblasts as regulators of PDL width [39]. For example, heat killing of PDL cells induces ankylosis [46]. In vitro studies have shown that PDL fibroblasts can inhibit mineralized bone nodule formation by rat bone stromal cells and one mechanism may be through the secretion of prostaglandins which inhibit bone formation [47]. Other cells also may contribute to the regulation of the PDL boundaries. The presence of the epithelial cell rests of Malassez may have a role in maintaining the width of the PDL space, possibly through secreting factors that promote bone resorption [48].

Populations of cells within the PDL, both during development and during regeneration, can secrete other molecules that can regulate the extent of mineralization and prevent the fusion of tooth root with surrounding bone, e.g. ankylosis. Among these molecules, a balance between the activities of bone sialoprotein and osteopontin may contribute to establishing and maintaining an unmineralized PDL region. Matrix Gla protein is also present in periodontal tissues. Based on its role as an inhibitor of mineralization, it may also act to preserve the PDL width [6].

At the genetic level, in vitro cell culture has shown that *Msx2* gene prevents the osteogenic differentiation of mouse PDL fibroblasts by repressing *Runx2* transcriptional activity. *Msx2* may play a central role in preventing ligaments and tendons, in general, from mineralizing [49]. Overall, the factors that trigger the various events in periodontal width homeostasis during tooth migration and orthodontic tooth movement still need to be ascertained [6].

5.1.2.4 Gingiva

Gingival epithelium has a protective role in resisting the insults produced by bacteria, chemicals, and trauma and plays a role in tooth attachment through the collagen fibre groups within the gingiva.

The free and attached marginal gingiva and sulcular epithelium are covered by a stratified squamous epithelium. Approximately 60-65% of the connective tissue compartment of healthy gingiva is occupied by collagen, with the individual fibrils organized into discrete fibre bundles. These gingival fibres provide tone and resistance to the free gingival margin and provide the most coronally positioned connective tissue attachment to the tooth surface [1].

5.1.3 Features of the periodontium unique to rodents

Rats have a monophyodont dental pattern with the incisors and molar teeth separated by a wide interdental space (diastema). The absence of a secondary dentition may also predispose to the prevalence of root resorption observed in rat molars [50]. The nomenclature for the upper first molar is M^1 and the lower first molar is M_1. The rat dental formula is I^1_1, M^1_1, M^2_2, M^3_3. The size of the molars decreases from M^1 to M^3. M^1 has 5 roots, M^2 four, and M^3 three roots in the upper jaw. The molar teeth of the rat

migrate bucco-distally throughout its lifespan [18, 51, 52]. The mesial surface is predominantly formative while the distal is more resorptive [20].

Unlike the repair of resorption lacunae in human teeth with cellular intrinsic fibre cementum [13], rodents may have acellular cementum [34] or cellular cementum [53] deposited within these resorptive defects. Kimura et al [34] hypothesized that this may be because cementoblasts in rats have a relatively high level of activity.

Therefore, certain aspects of cementogenesis and cementum biology (such as attachment mode of cementum to dentine, the rate of cementum apposition) seem to differ between rodents and large mammals, including humans [54]. Data derived from animal models must be used with caution before conclusions for human applications are drawn [41].

5.2 DENTINE-PULP COMPLEX

5.2.1 Dentine types-Response of pulp to dental trauma

A discussion of dentine types has been included to facilitate a description of the changes seen in the pulp in this study. Most of the tooth is formed by primary dentine, which outlines the pulp chamber. Secondary dentine develops after root formation is complete and represents a continuing, but much slower deposition of dentine.

Tertiary dentine is produced in reaction to noxious stimuli. This may induce the formation of reactionary dentine and/or reparative dentine [55]. Reactionary dentine is formed by the upregulation of the secretory activity of existing odontoblasts which survive the injury. As such, the injury to the tooth tends to be of a mild intensity. The presence of tubular continuity among primary, secondary and tertiary dentine may suggest formation by pre-existing odontoblasts. Reparative dentine is formed by the differentiation of new odontoblasts from certain cells within the pulp, in response to

localized odontoblast death. These include the fibroblasts, undifferentiated mesenchymal cells from the pulp core and vascular derived pericytes, which are potential sources of skeletal stem cells [27]. While pluripotent human adult stem cells have recently been extracted from the dental pulp [56], which differentiate into osteoblast precursors in vitro, the differentiation lineages of the stem cell population types within each of the above cell groups, in response to stimuli, has not been identified [55].

Tate et al [57], noted that the extent of the damage to odontoblasts may also determine whether intrapulpal bone-like tissue or tertiary dentine is formed. In a study of irradiated rat molars, he noted a reciprocal positional relationship between the intrapulpal presence of tertiary dentine and bone-like tissue, characterized by the presence of ostecyte-like cells in situ and the absence of dentinal tubules. Bone-like tissue was more prevalent in rats that received a higher intensity irradiation to their molars. Within the pulp of these rats, there was also a preferential accumulation of the bone-like tissue towards the irradiated site. In contrast, tertiary dentine was less prevalent and was confined to the pulpal walls away from the irradiated site. Tate hypothesized the cells that form the bone-like tissue may be either derived from mesodermal cells in the dental pulp, which may differentiate into osteoblast-like cells, under pathological conditions where regulation is disturbed from the absence of odontoblasts and/or cranial neural-crest cells in the pulp.

Predentine is a layer of variable thickness (10μm-47μm) that lines the innermost (pulpal) portion of the dentine. It is unmineralised dentine matrix and stains less intensely than mineralized dentine. Predentine is thickest where active dentinogenesis is occurring. Its presence is important in maintaining the integrity of dentine, since when it is absent the mineralized dentine is vulnerable to resorption by odontoclasts [58].

5.2.2 Pulp stones

Pulp stones are frequently found in pulp tissue. They are discrete calcified masses. They may be singular or multiple in any tooth and are found more frequently at the orifice of the pulp chamber or within the root canal. They usually consist of concentric layers of mineralized tissue formed by surface accretion around blood thrombi, dead or dying cells or collagen fibres. Pulp stones containing tubules surrounded by cells resembling odontoblasts are rare [58].

5.3 ROOT RESORPTION

Root resorption refers to the breakdown, and subsequent loss of the root structure of the tooth. Root resorption may be internal or external, depending on whether the resorption process originates from the pulpal or periodontal side of the root face. Odontoclasts are the principal cells in root resorption [38]. In contrast to bone, the roots of teeth do not normally remodel. Therefore, fatigue damage of these heavily loaded structures accumulates over a lifetime [30].

Beneath the cementum, adjacent to root dentine, is a structureless zone that seals the peripheral end of the dentinal tubules. This is the intermediate cementum, which is hypercalcified and appears critical in preventing the apical development of inflammatory resorption in replanted teeth, possibly by forming a barrier against the egress of noxious agents from the dentinal tubules to the PDL [59]. However, in response to external pressure stimuli ie: during orthodontic tooth movement, the root's outer layers, the cementoblasts and the precementum (cementoid) reportedly provide a protective function to resorption. These layers might contain non collagenic materials that possess potent

anticollagenase properties [60]. Resorption of the mineralized dental tissues occurs if clastic cells obtain access by a break in this barrier [21, 53]. This unmineralized precementum layer also protects the root surface during physiologic tooth migration [21].

5.3.1 Classification of external root resorption

External root resorption can be classified into several types[38, 59]:

1. External resorption associated with traumatic injuries of which there are three types-
    - Surface resorption- a self-limited type of resorption with small resorptive defects and repair with cementum-like tissue on the external root surface and root canal wall as early as 1 week after the injury.
    - Inflammatory resorption- This is seen in more severe cases of trauma. This is characterized by resorption lacunae at the root surface containing inflammatory cells. Damage to the cementum progresses to involve the intermediate cementum layer. In pulps that become necrotic and infected, this allows the escape of bacterial by-products into the PDL space via the open dentinal tubules. These bacterial by-products become the stimulus for ongoing phagocytosis, causing inflammation and further root and bone resorption. In pulps which remain vital and uninflamed, resorption leading to repair will occur irrespective of the depth of the resorption cavity [59].
    - Replacement resorption- this refers to the resorption process where the tooth root becomes replaced by alveolar bone.
2. External resorption from pulp necrosis and periradicular pathosis is characterized by large areas of periapical bone resorption, without much apically resorbed dentine. This differs from the more rapid onset of inflammatory root resorption

associated with trauma. In a narrative review, Gunraj [38] stated this was attributed to the insulating effect of the intermediate cementum which remains unaffected when the pulpal infection and necrosis were not caused by trauma.

3. External resorption from pressure in the periodontal ligament. This can manifest in apical shortening of the root as a result of forces during orthodontic tooth movement, or direct pressure from pathological lesions.

5.3.2 Histopathogenesis

This is dependent on the nature of the insult (which influences the quality of the damage) and the extent of the damage to the PDL [61].

Andreasen [62], in a study based on the histological changes after the extraction-replantation of teeth in monkeys, observed the number of damaged cementoblasts on the root surface was significantly larger in regard to replacement resorption than to surface- and inflammatory resorption. The degree of damage to the cells in the PDL along the root surface was related to later root resorption. Based on his findings, Andreasen proposed the following theory for root resorption:

1. If the root resorption is superficial (ie: not reaching the dentinal tubules), the resorption cavity will be repaired with new cementum.
2. If the resorption is deep, two different processes may be observed:
    - If the root canal contains infected necrotic tissue or an infected leukocyte zone, inflammatory resorption will occur
    - If the root canal contains normal or inflamed pulp tissue, repair of the resorption cavity will take place with new cementum. This may also occur if the root canal contains sterile necrotic pulp tissue [63, 64].

3. Larger areas of damage to the periodontal ligament characterized by the small amount of surviving cells close to the root surface would elicit healing processes with replacement resorption and rapid osteogenesis, thus forming an ankylosis.

However, as the extraction-replantation model induces a different type and extent of cellular injury, this theory may not be able to be extrapolated to freezing models that induce resorption and ankylosis [65, 66].

The histological changes seen in experimental models using thermal stimulii to induce injury to the periodontium are discussed below:

Wesselink et al [67] studied the histological changes that developed around the molars and incisors of mice after a direct thermal insult to their periodontium (10 second cotton wool dabbed in liquid nitrogen to lateral surface of jaw). In all cases where root resorption was restricted to the acellular cementum layer, mononuclear cells instead of osteoclast-like cells were seen. Although their resorptive activity was not able to be determined, Wesselink suggested that a different cell type may be involved in the resorption of acellular cementum.

Dreyer et al [53], in a histological study on rats, developed an experimental model with reproducible aseptic root and bone resorption. This involved the direct application of a thermal freezing insult (dry ice) of varying duration to the rats' molar teeth. Root resorption was initiated between 2 and 7 days after the freezing injury accompanied by the presence of amorphous acellular areas of hyalinization within the ligament. Similiar results were confirmed by Shaboodien[68], who observed root resorption after molar freezing was maximal at the day 7 observation period and was principally located in the

interradicular and cervical regions of the tooth. At day 14, repair of resorption lacunae was taking place and ankylosis was present at the interradicular area. Repair of resorption lacunae was completed at day 28.

The repair process consisted of the deposition of cellular cementum within the resorption lacunae. In addition, some areas showed a cessation of active resorption and a reduction in clast cell presence. Cell death of odontoblasts was noted within the pulp chamber in the day 7 observation period with a ten minute duration of freezing. It was hypothesized that the thermal effects were conducted through the tooth to the external surfaces of the root to similarly affect the adjacent cells in the PDL. The subsequent degeneration of the adjacent structures of the PDL might, therefore, expose the root surfaces to resorptive attack. No evidence of an inflammatory cell infiltrate was noted in the PDL of experimental teeth [53].

Kimura et al [34] studied the histometric changes in root resorption activity around the distal roots during physiological drift of rodent molars. Root resorption was found to be a transient and reparative phenomenon, with few inflammatory cells, and classified as belonging to external surface resorption, although some lacunae were relatively deep into dentine. No resorptive activity was noted on the mesial side of the distal root of lower first molars, while the distal side only exhibited root resorption in the middle side of the distal root.

5.3.3 Repair of resorption

The attachment mechanism of cementum to dentine is of clinical relevance as pathological alterations and clinical interventions may influence the nature of the exposed root surface and hence the quality of the new attachment that forms when repair

cementum is deposited. The mechanism by which these hard tissues bind together during odontogenesis is the same for acellular extrinsic fibre cementum and cellular intrinsic fibre cementum[6].

In bone, where resorption and apposition occur throughout life, a cement line always separates the new from the old matrix. A corresponding line, the reversal line, has also been observed between repair cementum and the resorbed root surface [13].

5.3.3.1 Morphological changes

Bosshardt and Schroeder [13] analysed the ultrastructual and light microscopical changes in 15/100 human premolar teeth extracted for orthodontic reasons that showed signs of superficial resorption. The remaining 85 were used in other studies of human cementogenesis. 2/15 of the teeth had undergone orthodontic tooth movement. He described the histomorphological events in the repair of the resorption lacunae as follows:

1. Following root resorption, the odontoclasts withdraw from the resorbed root surface and the bottom of the Howship's lacuna left behind is lined by about 1-2µm thick seam of exposed collagen fibrils representing demineralized, residual dentinal matrix.
2. The periphery of the resorption lacuna becomes populated by mononuclear cells that closely adapt to the residual matrix
3. These mononuclear cells produce a collagenous fibre fringe(FF), the base of which is intermingled with the collagen fibrils of the residual dentinal matrix
4. Advanced stages of FF formation resemble the matrix of acellular extrinsic fibre cementum. Fibroblast-like cells, interspersed among the FF matrix, partition the extracellular space into discrete, fibre-containing compartments.

5. Following establishment of this fibre attachment, the junctional zone between the initial repair matrix (the FF) and the residual dentinal or cemental matrix attains strong basophilia and represents the reversal line.
6. Further apposition of repair matrix is usually performed by cementoblasts and results in the formation of cellular intrinsic fibre cementum.

Similar morphological changes were also noted in the repair of root resorption lacunae in rodents after the termination of orthodontic tooth movement [21, 69].

5.4 PHYSIOLOGIC TOOTH MIGRATION

Teeth and their supporting tissues have a lifelong ability to adapt to functional demands and hence drift through the alveolar process, a phenomenon known as physiologic tooth migration. During this process, both remodeling of the PDL and the alveolar bone occur. The turnover rate of the PDL is not uniform throughout the ligament, with cells being more active on the bone side than near the root cementum. Therefore, the major remodeling takes place near the alveolar bone. In addition, a slow apposition occurs on the cementum surface throughout life [21].

5.4.1 Bone Kinetics

In rodents, as a result of physiologic distal drift [21, 52, 70], a constant and regular bone deposition without preceding resorption (bone modeling), is seen on the mesial side of the alveolar wall, with rapid remodeling of the alveolar wall on the distal side characterized by a continuous cyclic activation-resorption-formation activity[18, 20]. Differences in the rate of bone remodeling are also seen with age (see section 5.4.2.3). Periosteal modeling also helps to maintain the cortical thickness of the alveolar crest during the drifting of the tooth [18, 30, 71].

While there is a decline in bone formation and resorption levels with age [9, 51], marked increases in alveolar bone turnover were seen in response orthodontic tooth movement [51]. This demonstrates the dynamic ability of the supporting periodontium to maintain the tooth in response to different functional stresses.

5.4.2 Bone remodeling

Bone remodeling involves the coordination of cellular activities of two distinct lineages, the osteoblasts and the osteoclasts, which form and resorb the mineralized connective tissues of bone, respectively. Regulation of bone remodeling is a complex process involving hormones and local factors acting in an autocrine and/or paracrine manner on the generation and activity of differentiated bone cells. Clinically, the rapid remodeling of alveolar bone facilitates movement of teeth within the jaw bone by the application of orthodontic forces. However, the application of force on bone tissues can also influence the remodeling rate [17].

Generally, the remodeling process of alveolar bone is similar to that of trabecular bone [20, 72, 73], with remodeling sites undergoing an activation, resorption, reversal and formation sequence (see section 5.4.2.1). Within the periodontium, at any specific time, adjacent foci are asynchronous at different stages of activity, so that the PDL attachment is lost only focally and for short periods of time [6, 18-20, 71]. Soon after, new synthesis of PDL by fibroblasts with new alveolar bone production by osteoblasts collectively allow for reattachment at these remodeled sites. Asynchronous remodeling of the alveolar bone allows for the maintenance of a high level of anchorage of the tooth [17].

5.4.2.1 Cellular dynamics- the resorbing side

This side of the alveolar bone socket undergoes a continuous cyclic activation-resorption-formation activity, and is called the remodeling side [20]. The process of bone remodeling consists of periods of 1) resorption, 2) reversal, 3) formation, and 4) resting [18]. The remodeling cycle in the alveolar bone of 8 week old male rats has a duration of 11 days. This consists of a resorption phase of approximately 1.5 days, a reversal phase of 3.5 days, a formation phase of 1 day and a resting phase of 5 days [20]. A similar duration of the resorption phase was observed in the rat trabecular bone, suggesting similar characteristics of active osteoclasts in these two sites [72].

In the activation process, the bone surface is converted from a quiescent stage to the active resorption stage. The initiating factor is unknown, but is hypothesized to occur partly in response to local structural, metabolic, mechanical and nonmechanical requirements, upon which the osteocytes, acting as mechanosensors, produce an activation signal to initiate the bone remodeling process. This signal induces the ingrowth of capillaries, from which the mononucleated precursors of osteoclasts migrate to the region. The signal also stimulates the bone lining cells to contract and release factors that digest the underlying osteoid layer, exposing the mineralized surface for osteoclastic resorption. RANKL from osteoblastic cells binds to its receptor RANK on osteoclastic precursors, initiating the osteoclastogenic process. Thereafter, multinucleated osteoclasts are formed by the fusion of mononucleated precursor cells. The mature osteoclasts then migrate and attach to the exposed mineralized surfaces, becoming activated in the process and initiating the resorption process [19]. The asynchronous nature of alveolar bone remodeling makes it difficult to observe the activation process, as it is difficult to predict

where and when a group of osteoclasts will start to differentiate and actively resorb the bone [71].

In the resorption phase, osteoclasts remove a local packet of bone. The osteoclasts excavate the layer of bundle bone, pass through the cement line and resorb the surrounding bone, resulting in the local detachment of the PDL fibre bundles at their point of insertion into bone. On the resorbing side of the tooth, only minute amounts of bone are formed per cycle in the lacunae, so that the bone balance remains markedly negative [18]. The most commonly seen stage in rat alveolar bone is the quiescent or resting state. Approximately 47% of the resorbing side in the buccal root of the rat's lower first molar tooth is in this resting state [20]. Thus, the attachment is lost within the resorption lacunae and in small parts of the reversal foci for only small periods of time. About 10% of the resorbing side is in active resorption in young rats. This temporary focal loss of attachment is of no clinical significance to the tooth mobility. However, similar morphometric data are not available for human teeth during tooth migration [18]. At the end of the resorption phase, the osteoclasts withdraw and the reversal phase begins [18].

During the reversal phase, coupling of the resorption and formation sequence occurs. The frequency of Howship's lacunae without osteoclasts becomes 3 times higher than the extent of lacunae with osteoclasts. Mononucleated phagocyte-like cells come into contact with the bone surface and may complete the resorption and deepen the lacunae. The reversal lacunae are thus characterized by Howship's lacunae without osteoclasts and without osteoid tissue, lined with mononucleated cells [20, 71]. The next step is the formation of the 'cement line' (also known as reversal line) that records the exact limit

reached by resorption. It marks the interface between new and old bone and is typically scalloped [18, 19]. Fibroblastic cells attracted to the lacunae during reversal line formation secrete thin collagen fibrils in contact with it.

In the formation phase, osteoblasts align between the reconstituted fibre bundles and secrete bone matrix in the resorption bay to embed these fibres. Mineralization firmly anchors the peripheral part of Sharpey's fibres in the new bone. At the completion of bone formation, a resting phase of variable duration takes place until the functional conditions locally activate a new cycle, during which more bone is removed to accommodate further migration of the tooth.

Normal bone remodeling depends on a delicate balance between bone formation and bone resorption. RANK (Receptor Activator of nuclear factor-kappa) and its ligand RANK-L, members of the tumor necrosis factor family of receptors, are directly involved in the differentiation of osteoclast precursors and activation and survival of osteoclasts. RANK-L is expressed by bone marrow stromal cells, osteoblasts, and fibroblasts, while RANK is expressed by osteoclast precursors and mature osteoclasts. The binding of RANK and RANK-L induces osteoclast differentiation and activity. Osteoprotegerin, which is produced by bone marrow stromal cells, osteoblasts, and periodontal ligament fibroblasts, however, competes for this binding and functions as a soluble decoy receptor for RANK-L. Thus, osteoprotegerin is a natural inhibitor of osteoclast differentiation and activation. Any interference with this system can shift the balance towards increased bone formation or resorption. Pro-inflammatory cytokines such as IL-1 and TNF-α, two important players in periodontal bone loss, regulate the expression of RANK-L and osteoprotegerin [6].

.

5.4.2.2 Cellular dynamics- the apposition side

On the apposition side, the no longer functional bundle bone is resorbed from the endosteum and is replaced by lamellar bone, through the remodeling processes described in section 5.4.2.1. A cement line always separates the endosteal bone from the functional bundle bone.

The apposition side is mainly characterized by the presence of a continuous prominent row of osteoblastic cells that lie between the Sharpey's fibres over a layer of osteoid tissue. The bone balance is highly positive on this surface and under physiological conditions, the amount of bone deposited along the apposition side equalizes the net bone removed at the resorbing side [18].

Bone formation occurs in two distinct stages: matrix formation and mineralization [19]. During matrix formation, osteoblasts synthesize a mixture of molecules, including collagen, that are secreted into the extracellular environment where they constitute a seam of unmineralized bone matrix, the osteoid. The mineralization process occurs only in the mature bone matrix in which the gap regions are ready for hydroxyapatite deposition. As the osteoid matures, osteocytes regulate an influx of mineral ions from extracellular fluid to form hydroxyapatite crystals which are then deposited into the stabilized gap regions of the osteoid. The mineralization process starts at the mineralization front, which is the interface between mineralized bone and unmineralized osteoid, where the matrix is mature and in which fluorescent dye markers become incorporated. This process then advances towards the outer layers of bone as their maturation completes. A mineralization lag time of about 10 days in humans is required

for matrix maturation. This results in the existence of a 7-10μm thick layer of immature osteoid (the osteoid seam) which is frequently observed at the active bone forming sites between the mineralization front and the surface osteoblast layer. Upon completion of bone formation, a 1μm layer of unmineralized matrix remains on the bone surface [19].

5.4.2.3 Modifying factors

These may have an effect on the resorption or formation processes or both and certain factors with a greater relevance in relation to this research are discussed below.

1. ***Age.***

   In vivo studies in rodents using bone labels on both alveolar bone[9, 51, 74] and trabecular bone [72] have shown bone turnover decreases rapidly with advancing age. Baron et al [72] analyzed bone remodeling activity in the vertebrae of 8 week old male rats compared with 12 week old male rats. He found that despite a similar trabecular bone volume, younger animals had a five times higher bone formation rate and five times more osteoclasts than mature animals. He concluded that skeletal maturation in the rat profoundly affects remodeling activity. However, in both these two age groups, there was an equilibrated balance between bone formation and bone resorption that maintained trabecular bone volume.

   Similar observations on the decline in bone formation on the mesial surface (the apposition side) of molars towards the levels on the distal surface (the resorption side) of rats with advancing age were found by Misawa et al [9]and King et al[52]. A decline trend in the percentage of resorptive surfaces on the distal surface towards that on the mesial surface was also noted by Misawa et al [9], who studied alveolar bone turnover in rats from 6 to 100 weeks of age. These observations account for the continuous

physiological drift of teeth, though at a declining rate with age [18], with attrition one of the determinants of tooth movement in the later age groups.

In the young human adult, remodeling activity keeps bone mass relatively constant but, with advancing age, the turnover process appears to become gradually uncoupled. This has been generally attributed to a decline in bone formation due to decreased osteoblastic function, resulting in a relative excess of bone resorption, leading to net bone loss [9, 25].

Site variations

Within the alveolar socket wall in rats, the interradicular area, alveolar bone crest, and apical regions are normally active sites of mineral apposition [51, 74]. Both the intensity and mineral apposition in these sites were significantly reduced in the 60 week old rats compared to 13 week old rats, suggesting mineral apposition was also subject to decreases in bone remodeling rate with age. The periosteal surface of alveolar bone is a site of continuous bone formation, with usually no signs of osteoclastic bone resorption [71],[74].

2. Other factors

These can be categorized into systemic hormones (parathyroid hormone, vitamin D, calcitonin, estrogen etc), local factors (prostaglandins, growth factors and cytokines) and miscellaneous agents (ie: stress, calcium, phosphate, fluoride, immobilization and bisphosphonates). Bisphosphonates interfere with periodontal homeostasis through the intracellular uptake by osteoclasts and odontoclasts, which inhibits their resorptive function and shortens their lifespan[75, 76].

All have varying effects on the bone resorption and/or bone formation processes[25] but are beyond the scope of this research.

5.4.2.4 Regional Acceleratory Phenomenon (RAP)

RAP is an increase in all metabolic activities in the affected region of the body (including bone remodeling) as a result of injury or noxious stimuli. These stimuli may be part of a procedure in an experiment and may act as a confounding factor [77]. Subsequent processes associated with healing or repair may result in falsely elevated kinetic turnover indices and biased resorption and formation indices that do not accurately reflect the status of bone remodeling [78].

Within an experimental design, comparisons between the contralateral control side of a treated group with an untreated group would allow for an assessment of RAP on the bone responses[79].

5.5 ANKYLOSIS

Tooth ankylosis may be defined as a fusion of cementum or dentine with the alveolar bone [80].

A failure or alteration in the PDL must precede tooth ankylosis [81]. As long as the PDL intervening between tooth and bone is normal and intact, there can be no ankylosis. Once ankylosed, the connective tissue derivatives of cementum, dentine and PDL all tend ultimately to be replaced by bone [82].

Lindskog & Blomlof [83] proposed that ankylosis may be regarded as the only possible healing reaction when the balance between the expression of cementoblast-like and osteoblast-like phenotypes favored the latter and may be regarded as scar tissue formation (instead of repair or regeneration). Andersson et al[80], in an extraction-replantation model of monkey incisors, found a clinical diagnosis of ankylosis was possible by means of the mobility and percussion tests when 20% or more of the incisor root surface was involved, as confirmed by histological assessment. He found that radiographic examination was even less useful for the diagnosis of ankylosis of multi-rooted teeth. He concluded that when less than 20% of the root surface was involved, a correct diagnosis seemed impossible with clinical methods. In a small sample of human permanent molars with clinical signs of ankylosis (based on solid, clear sound and partial absence of the PDL space), more than 40% of the root surface was ankylotic when confirmed by light microscopy [84].

5.5.1 Experimental models

The most consistent experimental model in animals in which ankylosis has been studied is the extraction-replantation model [81, 82, 85, 86]. Other animal models that have been used include the use of a soldering iron tip into the prepared root canals of monkeys, to induce thermal injury to the PDL cells [46]. Cellular devitalization of the PDL by freezing using liquid nitrogen via a cryoprobe [65, 66] or soaked in cotton wool[67] and surgically induced damage to the periodontium [87] are other models using thermal and/or mechanical means in animals to induce ankylosis. Chemical models using prolonged administration of bisphosphonates in mice have also been used to induce localized ankylosis in rats [88, 89].

A consistent model to induce ankylosis is required to follow the events preceding and subsequent to ankylosis with assurance. Shaboodien[68] used Dreyer et al's aseptic root resorption model [53] of direct freezing of the rat molar tooth for a continuous duration of 20 minutes. He showed that ankylosis at the interradicular site was a reliable feature in all experimental rat molars from the day 14 observation period to the last observation period of day 86. The thermal models for inducing ankylosis create site specific cellular death without significant structural alterations, and may be advantageous in studying periodontal healing, where results from the thermal models may not be comparable with surgical injury from the extraction-replantation of teeth [65, 66, 74].

5.5.2 Periodontal wound healing

The PDL contributes cells not only for its own repair but also to restore lost bone and cementum [6]. Melcher[90] proposed that cells of the PDL and their progeny possess the ability to inhibit osteogenesis. If after injury to a portion of the ligament, the connective tissue cells which repopulate the wound are from the progeny of the PDL cells, normal PDL structure develops. If a portion of the wound is colonized from a source outside the ligament, ankylosis may occur. This hypothesis was supported by the observation of Line[46] who used labeled cells (as a marker of cellular activity) to observe the origin of cells from 3-31 days subsequent to an induced thermal injury to the periodontium. Within the ankylotic area, the bone marrow channels were widened in the early time periods which seemed to suggest the bone marrow areas as the major repopulating sites in the events preceding the onset of ankylosis.

Tal and Stahl[65] also noted that in their freezing model in rats, the onset of ankylosis occurred at later time points and was preceded by significant cemental and dental

resorption and some resorption in the non-vital alveolar plate of bone, which was characterized by the presence of lacunae without osteocytes. The end point, in the restructure of the PDL, appeared to be ankylosis. Lindskog & Blomlof[83] analyzed the different mineralized tissues around the dental root of monkey incisors and premolars following treatment of different periodontal pathosis. Four distinctly different appearances of the mineralized tissue layers on the marginal dentine surfaces were described:

1. new cementum
2. non-attached bone-like tissue. After accounting for occasional artefactual splits between the dentine and the bone-like tissue during the histo-technical procedure, it appeared that this bone-like tissue was likely only loosely apposed to the dentine surface. On occasion, an intervening layer of tissue debris was seen towards the root surface. This indicated that the mineralized tissue had formed not directly on the dentine surface, but within the periodontal space, close to the root surface and only appeared associated with the root after an extended healing period. It was hypothesized that this may have been formed by cells with an osteoblast phenotype from the pool of undifferentiated mesenchymal cells in the PDL.
3. partly attached bone-like tissue
4. ankylosis preceded by root resorption

In teeth where the surgically damaged root surface is repaired with a layer of cementum, the origin of the cementoprogenitor cells and the molecular signals triggering their differentiation into cementoblasts is not known[54], although the epithelial rests of Malassez may have a role [48].

5.5.2.1 Role of the epithelial rests of Malassez

Epithelial remnants of Malassez were observed in close proximity to the PDL fibre bundles of non ankylosed teeth where the PDL had a normal or close to normal histological appearance [81]. It was hypothesized that the epithelial rests of Malassez may have a role in maintainence of the PDL space and was possibly an associated factor in the limitation of root resorption in replanted teeth with a vital PDL.

Isolated islands of epithelial cells, resembling epithelial rests of Malassez, were seen within the PDL space of monkey teeth with the first two forms of mineralized tissue (new cementum and non-attached bone-like tissue) with no histological signs of ankylosis [83]. Epithelial cells rests of Malassez might also be involved in mediating repair cementogenesis as clusters of cells displaying their typical characteristics were found in close association within the PDL during the repair of resorption lacunae [44, 48, 69].

5.5.3 Pathogenesis

Ankylosis originates when enamel, dentine or cementum becomes replaced by bone tissue as a direct extension from the alveolar bone. Pindborg [91] stated that ankylosis could only be established after preceding resorption of the dental hard tissues. In ankylosed teeth, active resorption processes ramifying deeply into dentine and newly formed bone were seen side by side. In a narrative review of ankylosis, Jacobs[92] stated that ankylosis arose because of damage to the cells on the root side of the PDL. Cells from the bone side of the PDL then migrate and resorb tooth substance.

In a longitudinal and cross-sectional histological study[81] of replanted incisors and premolars in monkeys and dogs, that received root canal treatment at baseline, the development of ankylosis was described as a process in which bone trabeculae formed on the socket wall and gradually grew across the PDL space to fuse with the root surface. Follow up observation periods varied from 8 days to 33 months. The bone trabeculae then united and formed a solid plate directly upon the intact cementum or the previously resorbed cementum or dentine.

Andreasen [86] studied the histological pattern of initial ankylosis in monkey incisors that were extracted and replanted after varying extraoral storage and handling. No root canal treatment was undertaken. Follow up observation periods ranged from 2 to 8 weeks though results were mainly reported for the 2 week observation period in this paper. Non extracted incisors were used as controls.

Two histological patterns of initial ankylosis were described at the 2 week period. The first type was characterized by a complete mineralization of the entire PDL, with the newly formed bone displaying few irregularly arranged osteocytes and no lamellae. The second type consisted of layers of bone deposited upon the root surface and the alveolar wall, with an intervening soft connective tissue zone. Bony bridges united these layers and demarcated soft tissue components. The thickness of bone deposition on the root surface was significantly more than the thickness of bone deposited on the alveolar socket wall.

The data from this study also suggested a decrease in the incidence of ankylosis (as seen histologically) over time, as the observation period increased from 2 weeks to 8 weeks, in

teeth which had been subjected to the lesser insult of immediate replantation. Similar observations where ankylosis was more frequent in the molar teeth of rats which had been subject to a longer period of thermal insult were also noted by Dreyer et al[93]. Dreyer observed dentoalveolar ankylosis in rats which had been subjected to multiple(three) continuous freezing episodes of 10 minutes duration. In contrast, no ankylosis was seen in rats that had been subjected to a single freezing episode of similar duration. However, in rats subjected to either a single or multiple (three), continuous freezing episodes of 20 minutes duration, ankylosis persisted until the last observation period of day 28. In rats which had received osteoprotegerin (a member of the tumour necrosis factor receptor family, which inhibits resorption by blocking the effects of factors that stimulate clast cell differentiation**)** as well as a 10 minute single freezing episode to their molars, he noted ankylosis occurred in all rats. Bone deposition did not appear to be an aggregational process from the crestal bone surface towards the tooth. The ankylosis appeared to progress from the root surface towards the crestal bone and appeared to stain like bone rather than dentine.

Hammarström et al [94] studied the initiation and progression of dentoalveolar ankylosis in replanted incisors and associated root resorption in an extraction-replantation model in monkeys. Observation periods varied from 2 days to 40 weeks. Using decalcified, step-serial sections and hematoxylin and eosin staining, the rate of development and increased prevalence of histological signs of ankylosis seemed to be related to a longer extra-oral storage time period. The authors observed that ankylosis started with the apposition of a bone-like tissue on the cementum surface and with mineralized areas in the middle of the PDL. The central part then fused with the newly formed hard tissue on the root surface and socket wall. In teeth with established dentoalveolar ankylosis, the dental root

became covered by osteoblasts and osteoclasts in continuity with endosteal cells outlining the marrow spaces of alveolar bone. Similar observations in the development of replacement resorption leading to ankylosis, where the connective tissue cells of the PDL do not participate in its repair, were also noted in other studies [45, 46].

None of the above studies[81, 86, 93, 94] used fluorescent dye markers which would have shown the appositional activity of the corresponding root and alveolar bone surfaces in areas of ankylosis. While bone labels have been used in the study of periodontal wound healing in dogs where ankylosis occurred as a infrequent finding, there has been no mention of the morphogenesis of ankylosis in that study [95]. The distinction between cementoblasts and osteoblasts on H&E stained sections (at the light micrograph level) and based upon their proximity to the corresponding root and alveolar bone surfaces[86, 96] may not be valid in areas of ankylosis.

5.5.4 Spatial distribution of ankylosis

In Andreasen's extraction-replantation model of incisors in monkeys [86], the apical portion of the root in both maxillary and mandibular incisors showed a significantly more frequent occurrence of ankylotic sites compared with the cervical half. Histological studies of ankylosis in molar teeth have found a high prevalence of ankylosis in the interradicular area, in both human[84, 91, 97] and rodent species [53, 68, 89]. These sites, as have been discussed earlier, are normally active sites of bone apposition [51, 74].

Rygh & Reitan [96] noted in a histological study of 22 extracted human 'submerged deciduous teeth' that all were ankylosed with areas of ankylosis noted in the bifurcation.

Dreyer et al [53] and Shaboodien [68], using a thermal model, found an increased prevalence of ankylosis in the interradicular site of the rat molar. In histological studies on secondarily retained permanent molars (characterized by the cessation of eruption of the tooth after emergence) in humans compared with controls, the areas of ankylosis were observed mainly in the bifurcation and interradicular root surface [84, 97].

5.5.5 Resorption and ankylosis

Loe & Waerhaug [81] found that although root resorption usually preceded the development of ankylosis, this was not a necessary stage. Their long-term experiments also showed that root resorption was not necessarily followed by ankylosis. In all teeth, resorption was most severe in the initial time period and was continuous throughout the observation period in teeth which had a more severe insult to the PDL (teeth subject to extra-oral air drying or mechanical removal of the PDL). In teeth where a vital PDL was maintained, this resorption was self limiting.

Wesselink et al [67] observed the changes in the periodontium of mice up to 32 days after a freezing insult. He noted the development of root resorption and ankylosis after 1-2 weeks. Between 12-32 days, the resorption lacunae on the root surface progressively increased in number and size. By 17 days, alveolar bone lined by osteoblasts had occupied large areas of the PDL space. Bone-like tissue had been deposited along both intact root surfaces and sometimes along the resorption lacunae of dentine. In the ankylotic areas, Howship's lacunae were occasionally observed with osteoclast-like cells present with their ruffled border in close proximity to where the three mineralized tissues (dentine, cementum and bone) adjoined each other. A highly irregular thin layer of mineralized material was also consistently deposited along the root surface of both

incisors and molars within a few days after cold application. Its formation was not associated with the close proximity of fibroblasts or cementoblasts which suggested the absence of cellular activity. Wesselink postulated this layer may have a role in the tentative mechanism by which root resorption is initiated, possibly by attracting phagocytes to the root surface by some chemotactic mechanism or inhibiting the release and/or activity of an anti-invasion factor from the underlying cementum. Tal et al[66], using a thermal insult to the exposed buccal alveolar plate in rats, also found a similar pattern in the development of areas of ankylosis. Initially (up to 3 days postfreezing), the alveolar plate became non-vital. Significant dental resorption bays, and some resorption in the nonvital alveolar plate were noted at the day 14 observation period. Ankylosis was observed at the remaining two, longer observation times of 5 and 7 weeks post-freezing where signs of apposition of new bone on devitalized bone and cellular-like cementum on the resorbed root surface were commonly seen.

In Shaboodien et al's[68] study on thermally induced dentoalveolar ankylosis in rats using dry ice, tartrate resistant acid phosphatase activity was minimal or not seen in areas of ankylosis. Osteoclast cell numbers at the day 28 observation period was also less than at the day 7 and 14 observation periods (though insufficient sample sizes did not allow testing for statistical significance). This suggested a decreased activity of resorption and the replacement of clastic cells by reparative cells. However, Dilulio et al[98], in a separate experiment using a similar freezing protocol, quantified the resorptive surface along the root surface and noted the extent of root resorption did not appear to change between day 7 and day 28, with active resorption observed at day 28.

Biederman [82] stated the condition of tooth ankylosis was progressive. This was based on his observation that the earlier the onset, the more severe and profound the clinical consequences. However, a transient type of ankylosis, as discussed below, has been noted in experimental teeth which have received a mild insult[87] or in the initial observation periods [85, 94]. In these studies, the ongoing viability of the PDL seems to be important in the initiation of resorptive processes to prevent the progression of ankylosis

5.5.6 Transient ankylosis

In an in vivo study, ankylosis induced in rat molar roots by means of surgical damage to the cervical vestibular bone, PDL and cementum was temporary and eliminated 21 days after surgery by resorption when viewed histologically [87]. The resorption apparently started from intact parts of the PDL located apical and coronal to the injured area, with the removal of newly-formed bone by osteoclasts. This suggested the importance of a vital PDL in initiating repair processes.

In an extraction-replantation model of maxillary first molars in rats where teeth were stored extraorally in open air(dry) or sodium hypochlorite[85], ankylosis was verified initially by clinically established immobility. The molars where immobility established after 2 weeks was not present at 6 weeks were all subject to the shorter duration of 5 minutes extra-oral storage.

In Hammarström et al's[94] study on replanted monkey incisors, in the shorter extraoral time period of 15 minutes, a transient type of ankylosis was noted in the first weeks and was characterized by the formation of an immature 'callus-like' hard tissue in the PDL of most teeth. This newly-formed hard tissue seemed to regress with time, as it was not a

common finding in these teeth after longer observation periods. Hammarström hypothesized that the viability of the remaining PDL seemed to be critical for the regression of the ankylosis and its removal was similar in concept to the removal of calluses and the regaining of morphology and function after healing of a bone fracture.

Loe & Waerhaug [81] proposed that ankylosed teeth in 'moderate function', and in the presence of masticatory forces, undergo resorption as part of a response to reestablish a PDL space. This space is not maintained and new bone is formed in contact with the root surface, resulting in the progression of the ankylotic area. The joint effect of resorption and bone formation eventually leads to the replacement of the entire root by bone. This hypothesis was supported by the observations of Wesselink et al[88] who found, in mice, significantly greater root resorption, lesser area of ankylosis and more rapid regeneration of the PDL width around functional teeth compared to hypofunctional teeth in the observation periods after prolonged bisphosphonate administration. All the mice in the two longest observation periods had extensive resorptions of both root and bone that had resulted in the disappearance of all ankylotic areas. Wesselink suggested that in order to resolve areas of ankylosis and to reestablish a normal PDL, remodeling involving both bone and root resorption were required.

Andersson et al[99], in a study of the effect of normal masticatory stimulation on periodontal healing of replanted teeth in monkeys receiving a soft or hard diet, also found a significantly decreased incidence of ankylosis in the hard diet group. However, there were no significant differences in the surface root resorption between the two groups. He observed that masticatory stimulation seemed to partly prevent ankylotic fusion with the alveolar bone, rather than eliminating areas of established ankylosis. He hypothesized

that mechanical stimulation may have stimulated a rapid repopulation of necrotic areas of the PDL by blood vessels and fibroblasts, thus forming a functional PDL.

From the above studies, ankylotic fusion may be either transient or permanent, depending on the initial extent of the damage to the PDL. Andreasen[87], [62] postulated that in small injured areas, areas of temporary ankylosis could be resorbed by adjacent undamaged parts of the periodontal ligament and the new PDL replaces the ankylotic area. When the injured area is large, PDL cells would not be able to proliferate over the entire injured root surface and permanent dentoalveolar ankylosis results [62, 86, 94].

Hellsing et al [85] reported that it was reasonable to assume that the basic biological processes in the development of ankylosis and the associated root resorptions were similar in all animals. However, as discussed above, certain features of the periodontium are distinctly different between rats and humans and conclusions derived from rodent studies should not be inferred to apply for humans.

5.6 BONE HISTOMORPHOMETRY

Bone histomorphometry is a tool with which to gain insight into the processes of normal and abnormal bone physiology. In histomorphometry, there are directly measured variables and derived parameters of bone structure and dynamics. The assumptions of using derived indices are steady state remodeling and normal mineralization lag times[100].

Bone histomorphometry includes the measurement of morphologic components of bone ie: osteoid thickness, bone surface etc. These are static variables that are measured

directly. Histomorphometry can also estimate kinetic variables through the use of fluorescent labels, administered at timed intervals that integrate into forming bone. The distance between such labels provides information about the rate of bone formation and, by derivation, about other bone metabolic processes as well [101]. Its main clinical application is the quantification of different stages of the bone remodeling cycle, to provide an overview that would allow further investigation into molecular and cellular interactions.

Histomorphometric indices

The calculations and nomenclature of indices in bone histomorphometry are based on the definitions in Parfitt et al 1987 [100].

5.6.1 Applications

Dynamic histomorphometric techniques are able to assess the extent and duration of each phase of the remodeling sequence, and the cellular activity of both osteoclasts and osteoblasts [20].

Increases in the mineral appositional rate may suggest increases in osteoblastic activity at the cellular level, while increases in the active bone-forming surface may also suggest a greater number of osteoblasts producing bone, and thus of an increase in bone formation at the tissue level [102].

Bone resorption has been quantified statically in alveolar bone in terms of the number of osteoclasts (N.Oc/BS) and the percentage of the bone surface covered with osteoclasts (Oc.S/BS) [9, 52, 103, 104].

Proportion of resorptive surfaces (RS) has also been used to indicate resorptive activity [105]. This was determined by dividing the sum of the perimeters of the resorptive lacunae by the total perimeter of the measured area and expressed as a percentage. However, Parfitt et al [106] stated the terms 'formation surface' and 'resorption surfaces' should be avoided, and proposed the terms 'osteoid surface' and eroded surface' respectively. This was to minimize erroneous implications of current activity. Eroded surface (ES), also known as lacunar surface, comprises the osteoclast surface (Oc.S) and the reversal surface (Rv.S). Individual erosions could also be classified as osteoclast positive, ES(Oc+), or osteoclast negative, ES(Oc-). It is possible that some eroded surfaces covered by flat lining cells should be counted as quiescent surface rather than as reversal surface. [100]

5.6.2 Bone Labels

This is defined as any subsequently identifiable substance which deposits in bone tissue. [77]

5.6.3.1 Mechanism of action

When administered during the mineralization period, these calcium binding labels are deposited within the bone mineral during the time they are present in the circulation. The deposition occurs within the hydroxyapatite crystal lattice at the mineralization front [107]. At that point in time, the label instantaneously and permanently demarcates the osteoid tissue from the mineralized bone [108]. In the period of time between administration of the bone label and biopsy, additional unlabeled mineral is deposited which acts to 'cement' the label in place. It is thus secured from diffusing out, either in the body fluids in vivo or in the storage of fluids ex vivo [77].

5.6.3.2 Applications

Substances with fluorochrome properties that bind calcium are given to determine where and how fast bone is forming. The mineralized matrix secreted by osteoblasts contains calcium phosphate, which is detected by these bone labels. The use of two fluorochrome dyes as tissue time markers with a known time interval between them allows the determination of appositional rates [77]. There are several different kinds of fluorochrome dyes and various regimens are used in histomorphometric studies. Some examples of the vital dyes used are tetracycline, calcein, alizarin complexone and xylenol orange. These show different colours under fluorescence and have the advantage of giving sequential information when multiple labels are used [109].

In in-vivo experiments in rats using double labels, the presence of increased bone formative activity was suggested by the presence of 2 fluorescent labels as compared to only a single label [20]. When the labeled bone is decalcified, the bone labels are totally lost, so one must use undecalcified sections [107].

In assessing reproducibility of data, no significant differences were noted in any of the measurements {MAR(mineral apposition rate), BFR(bone formation rate) and MS/BS(mineralizing surface/bone surface)} between calcein (10mg/kg), alizarin complexone (25mg/kg), and xylenol (90mg/kg), where they were administered as a single fluorochrome in the rat's tibia [109]. No evidence of osteoblast suppression or increased periods of osteoblast inactivity was noted with any label, including tetracycline hydrochloride at 30mg/kg. The inhibitory effect upon bone mineralization of tetracycline occurred only with much higher dosages [109].

5.6.3.3 Limitations

A functional unit of bone created by the remodeling process, in which all cellular elements are involved ie: progenitors, lining cells, osteoclasts, osteocytes and osteoblasts**,** has been defined as a basic multicellular unit (BMU)[77]. Bone labels would only be detected if the labels fell onto active phases of matrix synthesis and mineralization at the BMU's.

For longitudinal sequential labeling, if the BMU's are in a formation phase of osteoid during the period between the labels, then any label incorporated into the rat during this period would not be detectable with fluorescent microscopy. This accounts for the appearance of only one marker in subjects whom have received two bone tissue time-markers. New BMU's begin mineralization between the two markers, thereby, taking the second marker but escaping the 'first', while others complete mineralization between the two markers, thus 'escaping' the second. This is known as the 'label escape' phenomenon[110]. With a longer mineralization time or a shorter time interval between labels, the proportion of double labels (to single labels) increase, which decreases the escape errors. However, a sufficient label interval is required to resolve the labels microscopically to obtain an interlabel width measurement. Parfitt[111] stated a marker interval of 6-8 days in a double labeling schedule is appropriate to minimizing labeling error.

Bone labels are preferably used to detect bone turnover in tissues with a higher turnover rate. A longer time interval would be required between administration of the bone label and biopsy, in low bone turnover sites, to allow adequate 'cementing' of the bone label.

Hence, bone labels become less useful in assessing bone deposition in older rats ie: 60 week old rats [51].

6. RATIONALE OF THE CURRENT STUDY

Ankylosis of a tooth stops its eruptive potential, leading to infra-occlusion of the affected tooth due to continued eruption of neighbouring teeth. An ankylosed tooth is incapable of tooth movement- eruptive, functional or orthodontic. In growing patients, progressive infraocclusion of teeth can produce significant aesthetic and functional defects. The aetiology of ankylosis is not known, but in all cases, there is a discontinuity in the PDL.

The aseptic root resorption model developed by Dreyer et al[53] has been shown by Shaboodien et al [68] to reliably produce ankylosis within the interradicular area of rat molar teeth at the day 14 and day 28 observation period, persisting up to the last observation period of 86 days. However, using the same model, Dilulio et al[98] found a decreased prevalence of ankylosis. He also noted a change in the morphology of ankylosis, with a trend towards diminishing areas of ankylotic union in the later time periods.

While the initial aim of the study was to assess mineralized tissue adaptation in the early stages of ankylosis, the results from Dilulio's et al[98] study suggested a resilient, dynamic nature of the periodontium in response to injury, and the repair responses within the periodontium would also be examined.

The use of vital bone markers in vivo at the day 7, day 14, day 21 and day 28 observation period would allow the quantity, direction and rate of mineralized tissue formation to be characterized along the bone, root and pulp surface, to further elucidate the dynamics of periodontal wound healing within this model, from the perspective of the mineralized tissues. Resorptive parameters would also be assessed at each of the four time periods

along the bone and root surface to demonstrate the turnover within this region and their relationship with the PDL width. Pulpal changes would be examined for any relationships with the concurrent changes in the periodontium.

The use of a single sham-untreated rat in each of the time periods would provide a broad overview of the nature of any regional acceleratory phenomenon, if present, in each of the observation periods.

7. AIMS

The aims of this study are:

1. to observe mineralized tissue adaptation, including dental resorption changes, subsequent to an experimental thermal insult within the interradicular region.
2. To investigate, through changes in the PDL width, if and how periodontal ligament homeostasis is disrupted in this thermal model.
3. To investigate, if and when ankylosis does occur, whether there is a regression with time.

7.1 NULL HYPOTHESIS

1. A single, prolonged thermal insult to a rat molar has no effect on mineralized tissue adaptation within the periodontium and pulp chamber.
2. The periodontal ligament width within the interradicular region does not change in response to this thermal trauma.

8 MATERIALS AND METHODS

8.1 Experimental animals

28 eight week old Sprague Dawley rats were obtained and randomly divided into four groups of seven animals corresponding to one of four observations periods ie: t_1= 7days, t_2= 14days, t_3= 21days, t_4= 28days. At t=0 days, six treatment animals in each group received a continuous 20 minute application of pellets of dry ice (CO_2 at -81^{0}C, BOC Gases, Adelaide, Australia) to their upper right maxillary molar crowns.

a) **First observation period t_1 of 7 days (Group 1)**

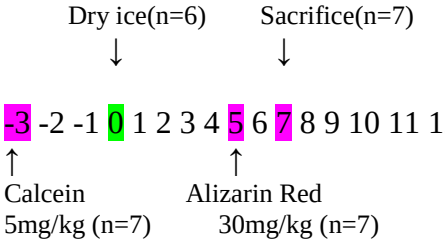

b) **Second observation period t_2 of 14 days (Group 2)**

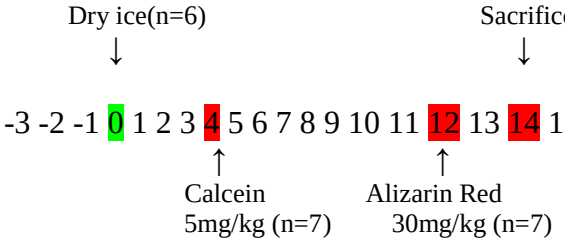

c) **Third observation period t_3 of 21 days (Group 3)**

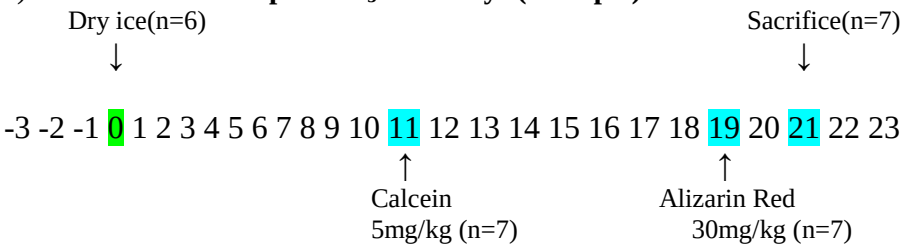

d) **Fourth observation period t_4 of 28 days (Group 4)**

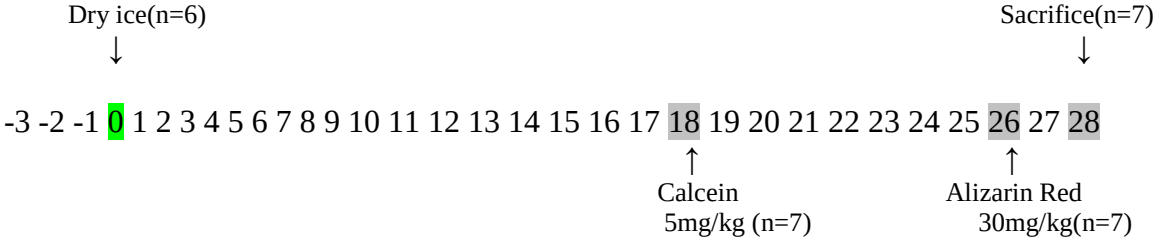

Figure 3. Diagram illustrating experimental design in rats in the 4 observation periods

The remaining single sham rat in each observation period did not receive the dry ice but had all other similar procedures with the treatment rats (Fig 3). This would provide an overview of any differences between the control side of the treatment rats and the sham rats, due to any regional acceleratory phenomenon effects on mineralized tissue remodeling.

All animals had their weights recorded at each of the above experimental time points: on the days of administration of dry ice, bone labels and on sacrifice. (Fig 4)

Figure 4. Digital scale balance used to record rat's weight

The animals were housed in the Animal House facility of the Medical School of the University of Adelaide and were fed a diet of commercially manufactured standard rodent pellets (Parastoc Feed, Ridley AgriProducts, Murray Bridge, Australia) and water, *ad libitum*. Approval of the experimental procedures was granted by the Ethics Committee of The University of Adelaide under ethics number M-054-2006.

8.2 Anaesthesia

Initial sedation was obtained by placing the treatment rats in each observation time period for several minutes in a gas chamber that received a continuous dual flow of isoflurane and oxygen. (Fig 5 & 6)

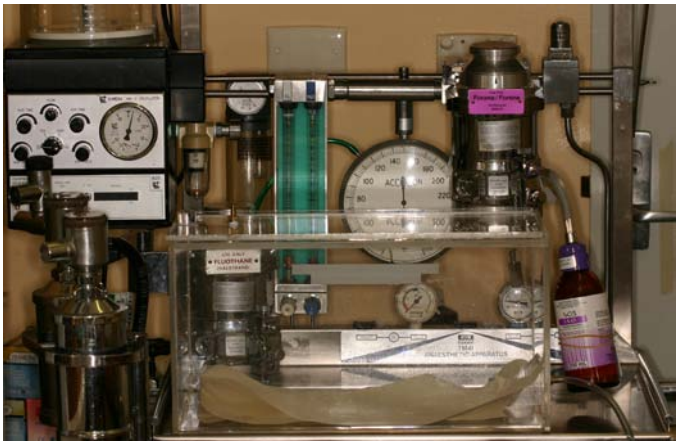

Figure 5. Isoflurane gas chamber

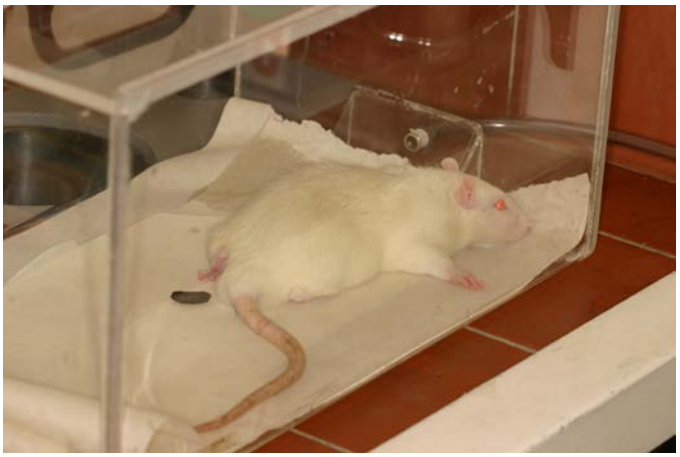

Figure 6. Inhalational sedation with isoflurane/oxygen mixture

The isoflurane reading was set between 2.5 and 3.0 depending on the initial weight of the rat. This provided a short lasting anaesthesia to allow the precise administration of an intraperitoneal injection of Ketamine (50mg/kg) and Xylazine (5mg/kg).

These rats were anaesthetized by the intraperitoneal injection of Ketamine (Ketamine Injection®, 100mg/ml, Troy Laboratories, Smithfield Australia) and muscle relaxant Xylazine (Xylazil®, 20mg/ml, Troy Laboratories, Smithfield Australia), administered intraperitoneally at a dosage of 2ml/kg of body weight. The two drugs were diluted with sterile water for injection. (Fig 7)

Figure 7. Elevation of rat's skin and superficial muscles to improve intraperitoneal administration

8.3 Thermal insult

Following Ketamine/Xylazine anaesthesia, individual rats were placed on their back on a specially constructed holding board, similar to a model used by previous studies [53, 98]. (Fig 8)

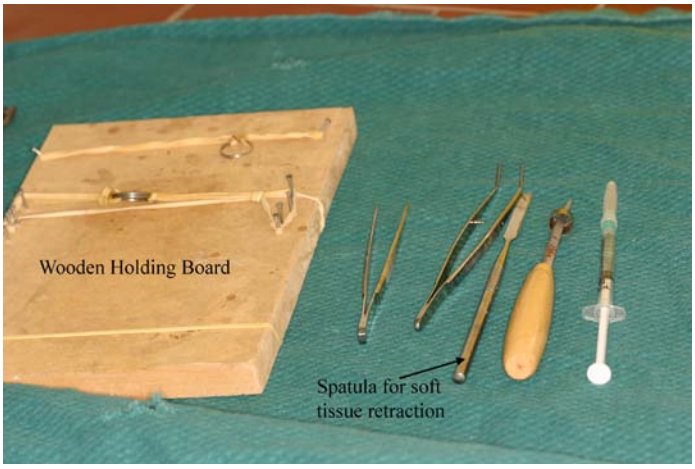

Figure 8. Armamentarium for dry ice administration in rats

The mouth was propped open by metal rings looped around the upper and lower incisors. The rings were individually attached by elastic bands to the support base so that there was a diametrically opposite pull on the incisors which gently stretched the mouth open. The tongue was positioned into the lower ring to protract it from the operative field. To expose the upper right first molar, a small spatula was used to retract the right cheek. The

restraining and retracting mechanism allowed one operator to perform the experimental procedures. (Fig 9)

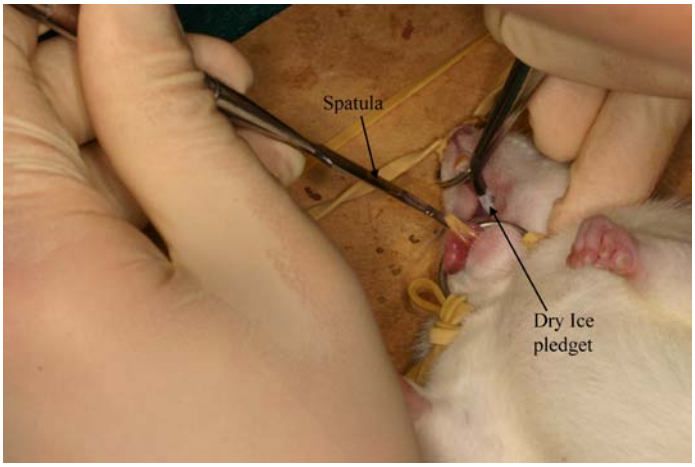

Figure 9. Anaesthetized experimental rat receiving dry ice to upper right first molar

The upper right first molar was frozen for twenty minutes by the continuous application of customized pellets of dry ice (CO_2 at -81^0C, BOC Gases, Adelaide, Australia) held in tweezers. Large tubular pellets provided by the manufacturer were divided using a sharp chisel producing smaller pellets with diameters approximating the crown size of the rat upper first molar. To avoid contact with the surrounding soft tissues, care was taken to apply the dry ice only to the occlusal aspect of the teeth. Following the application of cold, the tissues thawed slowly and the animals were allowed to recover. The upper left first molar was left unfrozen and served as a control.

During the post-operative recovery period, heat pads were used to keep the animals warm and where regaining of consciousness exceeded 1hour, 0.5ml subcutaneous sterile saline was administered to replenish fluids lost as a result of temporary loss of reflexes.

8.4 Bone Labels

Two bone labels (calcein, followed by alizarin red 8 days later) were administered intra-peritoneally to each rat according to the schedule in Fig 3. This was to allow sufficient

time for a physical separation of the mineralization front at the two time intervals and improve the contrast of the double labels when viewed with epifluorescence.
Calcein (calcein®, powder, Sigma-Aldrich) and alizarin red (alizarin red S®, powder, Sigma-Aldrich) were administered in solution at concentrations of 5mg/ml and 30mg/ml respectively. These were buffered to a neutral pH by dissolving in sterile 2% sodium bicarbonate solution. This was made by dissolving two grams of sodium bicarbonate with 100ml of sterile water. An acidic pH was avoided to minimize tissue damage to the surrounding tissues during administration of the bone labels.

Each rat's weight was recorded to calculate dosage and they were then sedated using an inhalational isoflurane/oxygen gas mixture. This provided a short-lasting sedation to allow controlled intraperitoneal administration of calcein (5mg/kg) or alizarin red (30mg/kg) at a dose of 1ml/kg of body weight.

8.5 Specimen collection

The four groups of seven animals each were euthanized via CO_2 asphyxiation at 7, 14, 21, 28 days respectively after the application of the dry ice. The maxilla was dissected out and trimmed, then immersed in fixative (70% ethanol) for several minutes before the enamel above the gingival sulcus was ground off using a diamond disc held parallel to the occlusal plane. The specimens were reimmersed in the same fixative. Care was taken to avoid dessication of tissues and to minimize damage to surrounding tissues during this disking process. The thermal insult, administration of bone labels and sacrifice all took place at similar times of the day in the morning.

8.6 Tissue processing

Tissue dehydration was carried out in 25ml polypropylene tubes with a graded ethanol series prior to defatting with acetone and infiltration with methylmethacrylate. These processes occurred within a vacuum chamber as part of the processing protocol. (Appendix 12.1)

During the final stage of addition of an initiator to commence polymerization, the tissue specimens were carefully oriented within the centre of the container base, to minimize the incorporation of bubbles during the polymerization process. The specimens were all mounted with the occlusal surface facing down to permit easy visualization of landmarks for sectioning with the container lids sealed tight and placed half immersed in a water bath held down by weights. Polymerization of the methylmethacrylate took place in a 37ºC oven for 2-3days.

8.7 Selecting region of interest- the representative furcation

An upper right rat molar from a deceased and frozen 8 week old male Sprague Dawley rat (which was not part of the author's original sample) was carefully extracted using a fine tip elevator to familiarize the principal author with the internal root anatomy. 5 roots were present, 3 buccal and 2 palatal, of which the mesiobuccal root was most prominent and extended some distance mesially. Scaled images were taken with a Leica MZ16FA stereo microscope. (Figs 10,11)

It was noted that if the crown of the upper first molar was divided into sagittal thirds, the middle third of the tooth would incorporate the region between the roots of the molars. The mesio-distal width of each third was approximately 1.0mm. This zone in the upper

interradicular region in the middle third of the crown was defined as the region of interest- the representative furcation. (Fig 12)

This provided a guide to the depth of sectioning with reference to the mesial surfaces of the upper first molars. A similar protocol was also adopted by Di lulio et al[98] in defining the central region of the first molar tooth as the 'furcation region.' The subsequent 1000μm was also disregarded as it mainly comprised the distal roots.

Figure 10. Upper right 1st molar of a Sprague-Dawley rat. Buccal view. Crown divided into thirds mesiodistally. MB: Mesiobuccal. Dotted line represents most mesial aspect of molar crown viewed from occlusal.

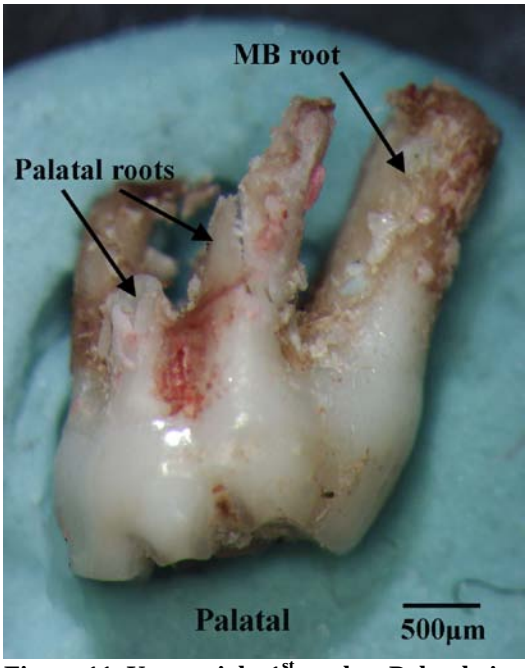

Figure 11. Upper right 1st molar. Palatal view. MB: Mesiobuccal.

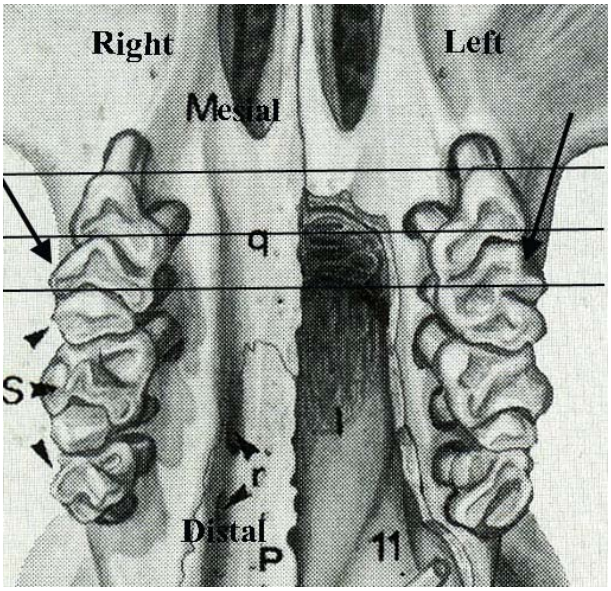

Figure 12. Diagrammatic view of occlusal surface of maxillary arch of male Sprague Dawley rat. [70]. Arrow denotes representative furcation of upper 1st molars in middle 1/3rd of crown.

8.8 Pilot study with micro-tomography

To facilitate an understanding of the 3D representation of the coronal sections obtained, images from a specimen block of the SHAM rat from Group 2 of the experimental rats, embedded in resin but prior to mounting on the aluminium stub, was subject to 3D scanning using micro CT with a Skyscan 1072. (Fig 13)

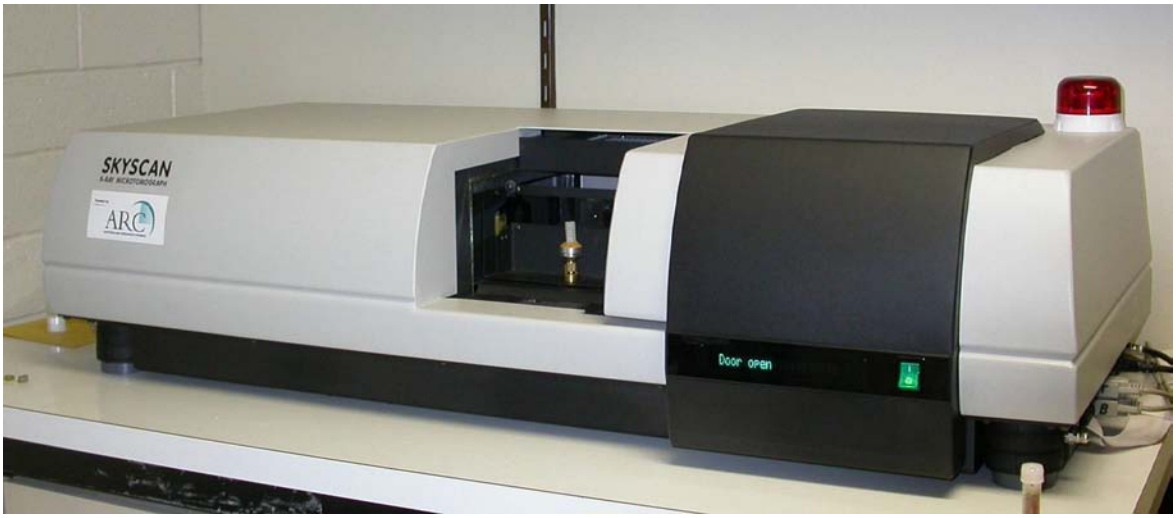

Figure 13. The SkyScan 1072, X-ray Micro-tomography system

The SkyScan 1072 is a compact desktop system which allows non-destructive three-dimensional reconstruction from the two- dimensional x-ray shadow projections. The SkyScan 1072 is a fourth generation scanner with a cone beam x-ray source with a maximum potential spatial resolution of 3 microns.

The specimen was placed on a rotating platform in front of the x-ray source and rotated through 180 degrees. Further detailed modifications prior to commencement of the x-ray beam, of the vertical height and amount of rotation of the specimen about its long axis, were able to be precisely controlled via digitally controlled manipulations of the metal base to which the specimen was attached with a stiff plasticine base. The raw data collected were reconstructed via SkyScan NRecon v1.4.4 software to provide an axial picture cross section. This software allowed two-dimensional images or slices based on the x-ray density to be recalculated from the x-ray shadow images. From the model, it was possible to make virtual cuts or slices of the maxilla in any direction.

The software program, Dataviewer version 1.3.2, was used to enable simultaneous visualization of axial, coronal and sagittal sections under interactive operator control.

This was used to reconstruct the collected data into viewable two-dimensional and three-dimensional images of the sample. The scanned image included the maxillary molars and the surrounding bone structure. The two-dimensional image could be manipulated to allow for optimal visualization of the region of interest (the representative furcation) and its macroscopic structural features.

8.9 Block preparation

The resin blocks were retrieved by sectioning the polypropylene tubes with a high speed band saw. Resin blocks were then grossly trimmed into rectangular blocks, where permitted by sufficient acrylic extensions, with the maxilla mounted supero-inferiorly, incorporating the 1st, 2nd and 3rd molars using a low speed diamond saw. In this way, the inferior base of the block corresponded to the side closest to upper 3rd molars' end of the maxilla. This orientation was necessary to obtain coronal sections of the upper right and left first molars of the maxilla with the Reichert-Jung microtome. Care was taken with the orientation of the blocks for sectioning so the inferior base of the block was flat and its superior surface approximated an imaginary line passing through the mesial aspect of the upper right and left first molars and was perpendicular to the occlusal plane.

The upper left corner of the resultant block was then filed off for orientation. In 6 specimen blocks (Group 1-rat 4, Group 2-rats 4 & 5 and Group 3- rats 1, 3, 6), the lower left corner was ground off to avoid proximity to the specimen.

The specimen blocks were then adhered to the aluminium stubs using epoxy adhesive with the side of the first molars lying furtherest from the stub base. In this way, with sections obtained from the block, the cut off corner would denote the right side of the rat

(excepting the 6 mentioned above). A marker pen was used to write the group allocation (Group 1, 2, 3 or 4) and the rat number on the base of the block.

8.10 Sectioning

The stubs provided the platform for mounting onto a Reichert-Jung microtome to allow 10μm serial sections to be cut through the furcation region. 10μm thickness sections were chosen as these would be thick enough to so that the calcium binding labels do not leach out with specimen processing techniques or have too short a shelf life yet thin enough for good cellular detail [74, 112]. With excessively thick sections, the spatial resolution of double labeling patterns reduces significantly. Yagishita et al[113] noted with 100μm sections, details of localization of bone marking labels became obscure due to superimposition of overlapping fluorescent images from many planes in the thick ground section.

The microtome permitted gross orientation of the specimen block in three dimensions, facilitating its positioning and sectioning. The aim in positioning and initial trimming was to have the cutting blade surface perpendicular to the maxillary occlusal plane and simultaneously approximate a line parallel to the mesial surfaces of the upper right and left first molars as closely as possible. Occasionally, small porosities on the occlusal surface of the maxilla made visual inspection of the mesial surfaces of first molar difficult. In these cases, a fine black marker pen was used to denote this reference prior to mounting onto the microtome. Precise initial orientation of the block was important to allow coronal sections to be cut, so that each section would include both the experimental and control teeth at the same depth. Subsequent repositioning of the stub which supported the specimen block during trimming had to be minimized as this often entailed

loss of additional specimen material. When the most mesial aspect of the upper right and left molar teeth was soon to be reached, as noted by visual inspection or by the black marker pen, the microtome blade was replaced with a sharper sectioning blade, with the microtome set to obtain 10µm thick sections.

When the mesial aspect of the upper right molar was reached, the number of sections was recorded. The first 100 sections were discarded as this was mainly the mesiobuccal root and not in the defined furcation as noted in Figures 10, 11 and 12. For the next 100 sections, each consecutive section was placed in a separate, prelabeled 5ml polyethylene tube and then tightly sealed and stored in a 10x10 foam test-tube block. The label consisted of the group number, rat number and the number of sections. In this way, a total of 100 consecutive, serial, coronal sections of the middle third of the upper first molar teeth were obtained from each of the 28 rat specimen blocks.

8.11 Processing of sections

The following protocols were derived from the Institute of Medical and Veterinary Science database and were used by the Bone and Joint Research Laboratory, Division of Tissue Pathology for undecalcified mineralized bone.

8.11.1 Slide preparation & mounting

Each of the above sections was mounted onto an individual gelatinized slide (Appendix 12.2.1).

Each section was spread onto a slide at 70ºC, using spreading solution (7 parts 70% ethanol and 3 parts 2-ethoxyethanol). The section was then covered with a protective sheet of plastic and a piece of filter paper to absorb excess solution. The slides were

numbered to enable orientation of the sections within the specimen. This process was repeated for each section.

They were then clamped together and allowed to dry in an oven set at 37°C for 2 days.

8.11.2 Staining

The first 3 in every 10 consecutive sections through the furcation were used in this study to provide a screening of the furcation region.

8.11.2.1 Unstained sections

The first series (in each 10 consecutive sections) were mounted and analyzed as unstained sections (Appendix 12.2.2).

This would provide information on the calcein and alizarin red bone labels when examined under epifluorescence with a Leica DM6000B microscope. The presence of bone labels on the bone or root surface would be indicative of instantaneous active mineralization of matrix.

8.11.2.2 von Kossa stain counterstained with H&E (VK/H&E)

The second series received a *VK/H&E* stain (Appendix 12.2.3). von Kossa stain contains silver which stains mineralized tissue black while the counterstain with hematoxylin and eosin stains the osteoid pink. As osteoid is the unmineralized matrix, the presence of osteoid can be seen when demarcated against a dark background of mineralized tissue[114], and would be indicative of an actively formative surface [18].

8.11.2.3 Haematoxylin and Eosin stain (decalcified sections)

The third series of each consecutive ten sections were decalcified by free-floating overnight in 10% EDTAC solution in 50ml transparent polypropylene containers before being mounted and stained with H&E (Appendix 12.2.4). This provided a morphological cellular overview, particularly of the mineralized tissues, not visible with the von Kossa stain counterstained with H&E. Sections were viewed under light microscopy using the Olympus CH microscope.

In this way, sections within each of the 3 groups (unstained group, VK/H&E and H&E) would be 100μm apart through the furcation region of interest.

8.12 Histomorphometry

8.12.1 Unstained sections:

Using a Leica DM600B microscope with a UV light source, the unstained sections were viewed firstly with the blue spectrum light (Excitation wavelength of 450-490nm). An optimal contrast of the labels was obtained at an exposure time between 8-13sec, with the lamp setting at 64.7%. This tended to differentiate the calcein label clearly while the alizarin red label stood out to a lesser extent. When viewed under the green spectrum light (Excitation wavelength of 515-560nm), the alizarin red label stood out strongly while the contrast of the calcein label was poor. Generally, the blue spectrum light was a better screen for the presence of both labels than the green spectrum light.

To obtain the best contrast of both labels, the images were viewed and captured using the 5x objective lens with the software Leica QWin Pro ver 3.3.1, using a personal computer

connected to the microscope camera. Images were recorded in pixels(px) with 1px= 1.07µm. Each section was initially viewed under the blue spectrum light, captured and saved, with the same process repeated under the green spectrum light. Using the Image J software ver 1.37 (National Institute of Health), the images (from each section) were then digitally merged and saved. As the field of view with the 5x objective lens was only sufficient to cover one tooth, the contralateral side of the maxilla had to be recorded and merged separately.

8.12.1.1 Quantitative analysis- developing a reproducible frame

A reproducible frame of reference was required in order to divide the tooth into vertical and horizontal regions which enabled comparisons between the control and experimental sides of the each animal within and between groups.

8.12.1.1.1 Grid size selection

Preliminary examination of the sections and of the scaled images of a rat molar tooth (Section 8.6) showed a 1000µm x1000 µm square grid would be sufficient to cover the representative furcation. Occasionally, marked mineral apposition was noted on the surfaces of the pulp chamber of the right molar which was not present on the left molar. The 1000µm x1000µm grid was also sufficient to extend to the pulpal floor of the pulp chamber. This grid was created using Adobe Photoshop (ver 8.0) (Fig 14). The grid area on the section was cropped, then enlarged using the Image J software for digital tracing (Fig 15). A 900µm x900µm grid had been used by Di lulio et al[98] in delineating the furcation as his region of interest.

8.12.1.1.2 Positioning the grid

The images from the micro CT represented the gold standard in specimen positioning as at the same depth of plane, the images of the right and left tooth were close to mirror images of each other. Preliminary analysis of the slices from the rat maxilla specimen block that had received micro CT showed that within the representative furcation, the cemento-enamel junction (CEJ) of the tooth and the pulp chamber were always present. As the middle roots of the rat were more diminutive than the mesial and distal roots, within the region of interest, occasionally, some slices had one root structure completely absent.

The structural features which defined the grid position were:

1. The centre of the grid was to be within the middle of the interdental septum of alveolar bone. It was one of the aims of data stratification to see if there were any differences between the buccal and palatal bone surfaces, so the long axis of the interdental septum and not the tooth was selected as the vertical frame of reference. The middle of the periodontal ligament (PDL) of the furcation area defined the horizontal frame of reference.
2. If only one tooth root was present on the section as well as the CEJ of the tooth and pulp chamber, then the buccolingual centre of the furcation surface of the tooth crown would be used in positioning the grid (Fig 14).
3. If the crown and pulp chamber were not identifiable or completely absent, or if both root structures were completely absent, the section was disregarded in data analysis.

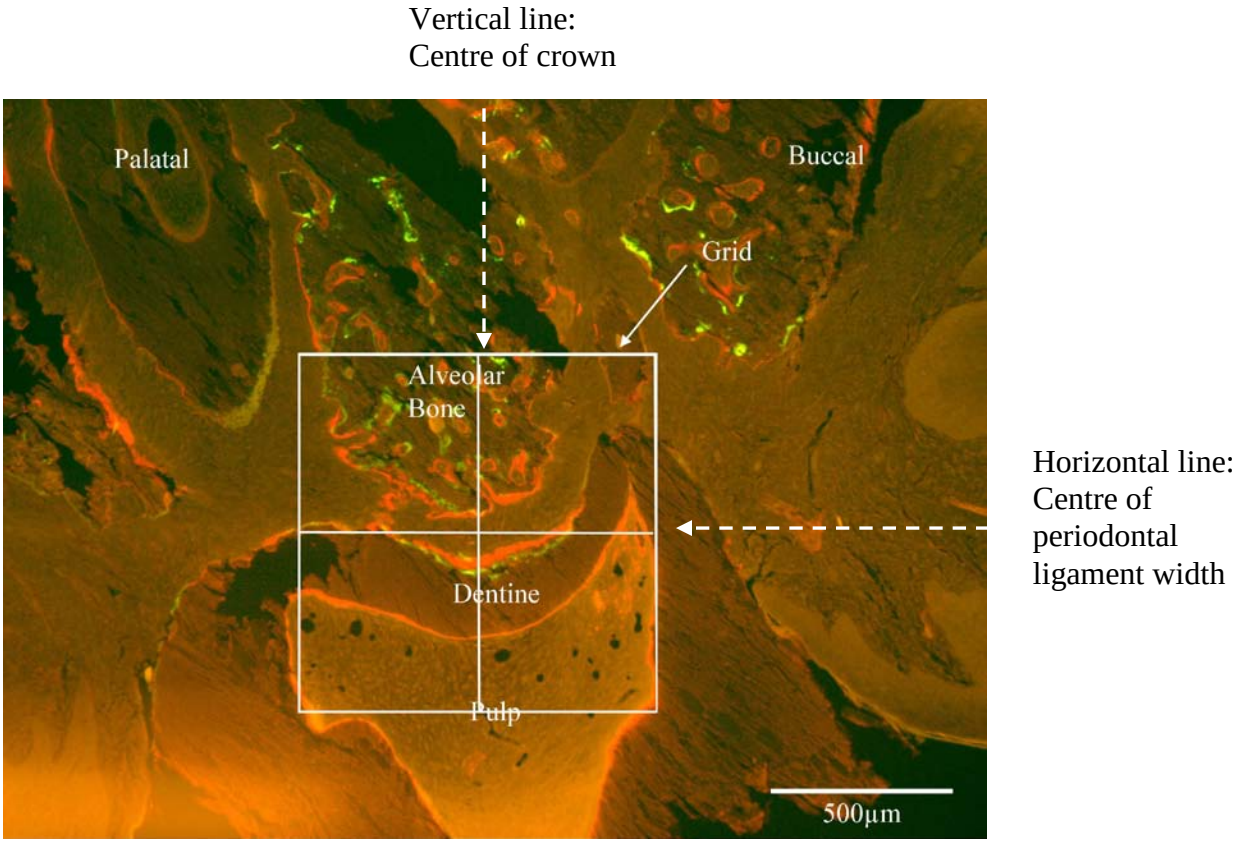

Figure 14. Square grid of 1000µm length, used for quantification in unstained sections, positioned using the centre of the crown and periodontal ligament width as guides

8.11.1.1.3 Measurement protocols

Preliminary examination of the sections showed there was a wide variation in the appearance of the labels. Sections varied from having no labels, one label only (either the calcein or alizarin red label), or both labels present. The labeling lines ranged from long continuous lines to short and interrupted lines. Due to this wide variation, the following protocol was adopted for the quantitative analysis (Fig 15):

- Only surface labels were to be measured. These were the surfaces on the bone and tooth which are closest to the periodontal ligament in the representative furcation
- In surfaces with multiple labels of different orientations, the longest unbroken label was measured (in region of no distortion).

- The most superficial surface of the bone label/s with respect to the PDL was taken as the reference surface for measurement.
- In sections where only one label was found, the distance from this to the peripheral bone surface (adjacent to the PDL) was also measured. This was denoted as 'modified mineral apposition rates' as mineral apposition rates (MAR) defined by Parfitt[100] required the simultaneous presence of the two labels, calcein and alizarin red.
- Results were stratified based on the presence of 1 or 2 labels and the label type (calcein or alizarin red).
- Measurements were disregarded in areas where there were tissue tear, folds, stretch or labeling lines that were indistinct

8.11.1.1.4 Measurement parameters

Within this grid, data analysis was divided into buccal and palatal halves. Quantitative analysis was undertaken using the Image J software with all tabulated data entered into a spreadsheet format using Microsoft Excel 2003.

For each of these 2 zones, mineral apposition rates or modified MAR (MAR_{mod}) were separately calculated for the bone, root and pulp surface. This was obtained by using a computer mouse with the arrow cursor which digitally delineated the area between the labels or surfaces (A_{ls}). The average length (L_{av}) of the labels or surfaces was recorded next. (Fig 15)

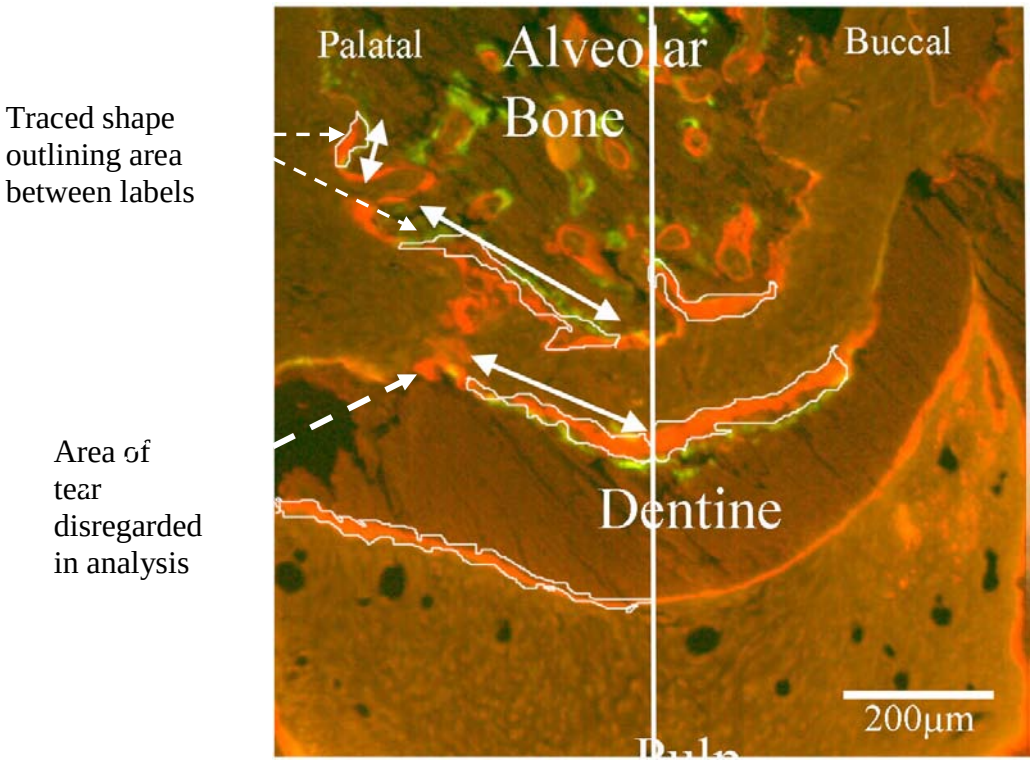

Figure 15. Only surface labels measured and traced. Cropped 1000µm x1000µm grid from Figure 14. Double –ended arrows denote the label lengths

The time period between administration of the two bone labels was 8 days. Measurements recorded in pixels were converted to µm using the conversion factor 1px=1.07µm. MAR was obtained as follows:

$$MAR\ (\mu m/day) = \{(A_{ls} / L_{av}) \times 1.07\} / 8$$

Values for MAR_{mod} were also obtained using the same formula. In the absence of a second label, time periods for the bone, root and pulp mineralized tissue surfaces were not possible. The same time period of 8 days was used with a view to further modification pending data analysis.

The periodontal ligament width (PDL_{width}) in these two zones was also recorded. This was first obtained by digitally delineating the area of the periodontal ligament (PDL_{area}). The average length (L_{bt}) of the bone and tooth surface was recorded next. PDL_{width} was obtained as follows:

$PDL_{width} = PDL_{area} / L_{bt}$

8.12.2 von Kossa counterstained with H&E sections

These sections were viewed under light microscopy using an Olympus CH microscope. A similar sized 1000µm x1000µm grid, derived from an eyepiece graticule, was used. The grid consisted of 10 x 10 squares, with each square 100µm x100µm (Fig 16). The same guidelines as for the unstained sections were used in positioning the grid over the furcation region in the section (section 8.12.1.1.2). As the grid position was fixed, positioning was controlled by moving the slides using the adjustment knobs.

8.12.2.1 Measurement parameters

Semiquantitative analysis using point counting was chosen as the method of analyzing bone and root resorption within the periodontium to assess relative differences between experimental and control 1st molars, and as a function of time. This involved measuring the following parameters on the bone and root surfaces adjacent to the PDL, within the 1000µm x1000µm grid, on both the right and left upper 1st molars:

1. The number of points where the intact resorptive surface (R_{bone} or R_{root}) intersected the vertical lines of the grid
2. The total number of points where an intact bone (T_{bone}) or root (T_{root}) surface intersected the vertical lines of the grid.
3. The total number of intact resorption lacunae (NL_{bone} or NL_{root})

In slides where sections were partially missing, torn, stretched, folded or had staining artifacts, counting was ignored where the vertical lines of the grids crossed these regions within the grid area. Counting as defined above continued in other unaffected parts of the slide. Structural features which assisted the identification of a resorptive surface were the

presence of ‘punched out appearances’ on the surfaces which suggested Howship’s lacunae, either with or without multinucleated cells, absence of an osteoid seam on the bone surface and absence of a lining of cells in the ‘punched out’ lacunae on the bone or root surface (Fig 16). Resorption as defined here refers to the resorption and reversal stages of the bone remodeling cycle [18, 20] or the root remodeling cycle during the repair of root resorption lacuna[13, 69, 115] .

Data were recorded into a spreadsheet format using Microsoft Excel 2003.

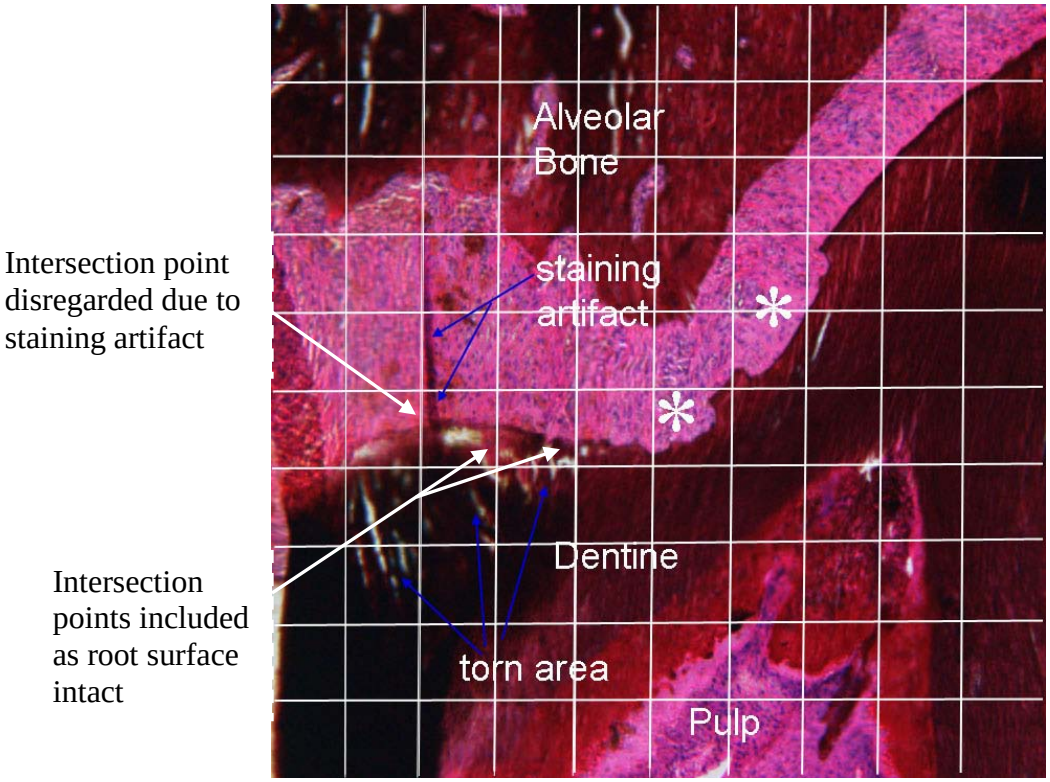

Figure 16. 1000µm x1000µm grid used for semiquantification of von Kossa counterstained with H&E sections. Asterisks denote ‘punched out’ appearance along dentine surface used to identify resorptive surfaces.

8.13 Microscopic imaging

Recording of the H&E and VK/H&E sections were carried out using the facilities of the Adelaide Microscopy Centre. Sections were viewed using an Olympus BX51 microscope with attached digital camera, and the areas of interest were examined using 10x, 20x and 40x objective lens. Image capture was carried out with AnalySIS LS Research imaging

software using a personal computer connected to the microscope camera. Adobe Photoshop CS ver 8.0 was used for adding labels and markers to all images to be included as figures within the text.

8.14 Statistical analysis

This was carried out using SAS Version 9.1 (SAS Institute Inc., Cary, NC, USA).

8.14.1 Mineral apposition rates and periodontal ligament width

The data for MAR and PDL width were first plotted as histograms to check if they were normally distributed. The MAR data had to be transformed into logarithm values (log MAR) to fit linear models, and then back transformed into mean MAR values. Since MAR_{bone}, MAR_{pulp} and MAR_{root} referred to the same outcome measured in different locations, models were run with log MAR as the outcome.

A linear mixed effects model was separately fitted to the log MAR data and PDL width data from all the 28 rats (treatment and sham). This used multivariate analysis, in which the influence of each variable on MAR was interpreted as its relationship after adjusting for all the other variables in the model.

For the outcome of mean MAR, the 6 variables examined were label types (presence of calcein and /or alizarin red labels), location (bone, root or pulp), time (days 7,14,21 or 28), side (left or right), aspect (buccal or palatal), and group (treatment or sham rat). Multiple interactions between MAR and combinations of the significant variables were also assessed.

For the outcome of mean PDL width, the 3 variables examined were time, side and groups.

8.14.2 Resorption

A negative binomial GEE (generalized estimating equations) model[116, 117] was fitted to the resorption data where the outcome was either resorptive surface ($R_{bone\ or\ root}$) or number of lacunae ($NL_{bone\ or\ root}$), with the logarithm of total intersection points ($T_{bone\ or\ root}$) as an offset variable. This approach was chosen due to the problems associated with modeling ratio variables which were not normally distributed. The adjusted means outcome was expressed as a rate and termed 'mean % of resorptive surface' or 'mean % number of lacunae'. The variables investigated were side (left or right), location (bone or root) and time (days 7,14,21 or 28). Multiple interactions were also assessed.

The relation between resorptive surfaces and number of lacunae, were also investigated using a similar negative binomial GEE model with resorptive surfaces as the outcome, adjusting for the additional variable of number of lacunae.

8.14.3 Method error

To investigate the reliability of the results, 6 rats were randomly selected for the error study two months after the first set of measurements. Remeasurements of MAR in the bone, root and pulp, PDL width, and $R_{bone\ or\ root}$, $T_{bone\ or\ root}$ were undertaken.

For MAR and PDL width, the Bland-Altman test[118] was used to examine reliability. As the reproducibility ratios for '% of resorptive surface' were not normally distributed, a symmetric Bland-Altman test was not appropriate. Boot strapping was used to estimate the limits for the resorption ratios. This is a type of resampling technique that estimates the precision of sample statistics by drawing randomly with replacement of 1000 or more data values [119].